Glass Europe Vol. 4 (2026) 29-61

https://doi.org/10.52825/glass-europe.v4i.3253

© Authors. This work is licensed under a Creative Commons Attribution 4.0 International License

Submitted: 27 Jan. 2026 | Accepted: 23 Mar. 2026| Published: 02 Apr. 2026

# On the Origin of Delayed Elasticity in Inorganic Glasses

Yann Gueguen[1,*]

[1]Univ Rennes, CNRS, IPR (Institut de Physique de Rennes)- UMR 6251, F-35000 Rennes, France

*Correspondence: Yann Gueguen, yann.gueguen@univ-rennes.fr

**Abstract.** Delayed elasticity is a universal feature of glasses, manifesting as a recoverable deformation accompanying viscous flow across the glass-transition domain. While heuristic models have been proposed to explain its origin, the underlying mechanisms remain poorly understood. Here, the origin of delayed elasticity is investigated using a mesoscopic shear transformation (ST) model within the linear viscoelastic regime. Glasses undergo continuous, thermally activated STs that generate long-range stress fields, leading to a randomly fluctuating internal stress. In the linear viscoelastic regime, applied macroscopic stresses are much smaller than the characteristic stress fluctuations induced by interactions between shear transformation zones (STZs). The model reveals that delayed elasticity emerges from the collective behavior of STZs rather than from their individual mechanical history which cannot be preserved under such fluctuating internal stresses. When STZs have no intrinsic distribution of energy barriers, localization into shear bands mays occur, leading to faster inelastic strain accumulation in certain regions and the generation of a certain counteracting ”back stress.” However, more realistically, when an intrinsic distribution of energy barriers exists, localization is suppressed, and delayed elasticity arises instead from the cooperative dynamics of STZs. The back stress, which drives delayed elasticity recovery, originates from these collective interactions, through long-range stress fields, rather than from individual mechanical history/memory. Thus, the memory behind delayed elasticity, often considered local, is fundamentally collective.

**Keywords:** Delayed Elasticity, Anelasticity, Glasses, Viscoelasticity, Shear Transformation

## 1. Introduction

In a large temperature range, below their Littleton softening point, and under relatively low stresses, all inorganic glasses behave as linear viscoelastic materials [1].

Meaning to say, their shear elastic moduli are still relatively high, and their viscosity still relatively low. Consequently, under stress, they will exhibit both elastic and non-elastic strains. The latter can be divided into two parts: the irreversible one, namely the viscous strain, and a strain that will continuously recover once the stress is removed, after the instantaneous elastic recovery, and thus originally named ”*elastic aftereffect*” [2], [3], [4]. The microscopic origin of this phenomenon is still not well understood.

## 1.1 Historical origins

This *aftereffect* still has various names in the literature, and this can be a source of confusion. For a long time, the discovery of this effect was considered [5] to have been made in Germany by Weber [6], [7] in the mid-19th century, but it can be assumed that Cavendish[1] had already observed and described this effect before the end of the 18th century (see also [9]), without understanding and naming it. When first "re-discovered" in Germany, it has been named in German "*Elastische Nachwirkung*" [7], [10], [11], [12], [13] [2]. The first article of Boltzmann on *der Elastische Nachwirkung*, being the foundation of linear viscoelasticity [18], was published in German in 1874 [11], and then in English two years later [2], with probably the first use of the terms "*elastic after-effect*", terms subsequently used for decades [19], [20], [21], and eventually translated as "*elastic after-working*" [22], [23], [24], [25], [26], [27], [28] (see [15] for information on when, where, and why these terminologies emerged). Griggs [29] introduced the terms "*elastic flow*" instead ("*elasto-viscous*" strain has also been used [30]), which would soon be roundly criticized by Washburn [31], but is still in use. The terms "*imperfect elasticity*" have also been used for this phenomenon [32], [33], but were very generic terms for any kind of non-elastic phenomena [34], such as plasticity [35]. Since at least the 1930s it is also named, for inorganic glasses, "*delayed elasticity*" [28], [36], [37], [38], [39], [40]. Then the term "*anelasticity*" is popularized by Zener [41] as *a "non permanent plastic deformation"*, first for metals, but interpreted as due to a viscoelastic deformation of amorphous grain boundaries [42]. It seems it has been applied to oxide glasses first by Fitzgerald [43], [44], [45], [46] and Hoffman [47]. Argon has used many of the terms mentioned above in his PhD thesis (as well as "*elastic creep*") [48] and in others of his work [49], but later used the term anelasticity for non-linear behaviors and delayed elasticity for linear ones [4]. It is less often (in the field of inorganic glasses) named "*retarded elasticity*" [15], [50]. In the 1960s oxide glass community, anelasticity referred to reaching strain equilibrium under creep, whereas delayed elasticity denoted recoverable deformation [51]. Nowadays, the term "anelasticity" is primarily used in the metallic glass community, while the term "delayed elasticity" is primarily used in the communities of other inorganic glasses, schematically.

## 1.2 Inelastic deformation in glasses

Glasses are often considered as archetypal brittle materials. However, it is now well established that they can also undergo inelastic (irreversible) deformation, even at room temperature. Under these conditions, the inelastic deformation is said plastic, meaning that a stress threshold must be exceeded in order to produce an irreversible strain [35], [52], [53]. Although plastic events are generally also thermally activated, when their activation is dominated by the applied stress rather than by temperature they are commonly referred to as *athermal* [54]. In many amorphous materials, including metallic glasses, it is now widely accepted that athermal plastic deformation originates from localized shear rearrangements involving small groups of atoms, or particles. These elementary events, usually called shear transformations (STs), correspond to localized plastic shear rearrangements whose amplitude is essentially independent of the applied stress [54], [55], [56], [57]. In oxide glasses, a well-known form of plastic deformation is densification [58], [59]. This process occurs above a certain pressure

[1] "*It must be observed, that if a wire is twisted only a little more than its elasticity admits of, then, instead of setting, as it is called, or acquiring a permanent twist all at once, it sets gradually, and, when it is left at liberty, it gradually loses part of that set which it acquired.*"[8]

[2] For background interest, the reader is referred to references [14], [15] on the rich history of the aftereffect, which has also been interpreted as a possible property of the famous ethereal medium [16], [17]

threshold and is associated with structural changes such as modifications of ring sizes and coordination numbers. Densification can also occur in metallic glasses, but to a much more limited extent [59]. Nevertheless, shear plasticity has also been reported in oxide glasses [60], [61], involving spatially heterogeneous and strongly localized mechanisms consistent with shear transformation-like events [62]. Shear banding has also been observed in silicate glasses [63], as in metallic glasses. When the temperature increases, glasses progressively become more ductile. This transition is generally associated with the onset of viscous flow [64], which corresponds to a thermally activated inelastic deformation. In metallic glasses, viscous flow is often assumed to also occur through shear transformations [54], [65]. In oxide glasses, however, direct evidence for such a mechanism remains limited. Goldstein proposed that viscous flow could be described as a sequence of local structural rearrangements between metastable configurations [50], and this description was not restricted to a particular type of glass and therefore suggests a certain degree of universality. A similar picture has been developed by Argon [40] for oxide glasses.

Below and within the glass transition range, glasses retain a high elastic stiffness while thermal energy remains relatively low. Under these conditions, it is reasonable to assume that local rearrangements occur individually within an essentially elastic matrix. It should nevertheless be emphasized that local ionic or molecular motions ($\beta$-relaxation) persist below the glass transition temperature [66], [67]. In the present work, such localized motions are not considered, and the discussion is instead restricted to the cooperative viscoelastic response of the network (associated with the $\alpha$-relaxation).

Following these ideas, I assume that, in the glass transition range, viscous deformation in oxide (or chalcogenide) glasses also involves thermally activated local rearrangements of a limited number of structural units, such as atoms, ions, polyhedra, or rings. These events would therefore correspond to quantified inelastic shear rearrangements: Because only a small number of atoms are involved in each rearrangement, the number of accessible stable configurations is expected to remain limited. This is particularly true since viscous flow does not change the thermodynamic state of the glass [50], and therefore does not significantly modify its overall structure. However, the present work does not address whether these rearrangements also dominate at room temperature or whether they are directly involved in the athermal plasticity of oxide glasses.

Under a purely deviatoric stress, the viscous flow of inorganic glasses is generally considered to be nearly volume-conservative. This suggests that the elementary rearrangements responsible for the flow correspond predominantly to shear transformations. At the microscopic scale, such rearrangements in metallic glasses may nevertheless include a small dilatational component, although shear remains the dominant contribution [54]. In contrast, when a hydrostatic pressure is applied, glasses exhibit a time-dependent and reversible decrease in volume [68] that remains finite, *i.e.*, under imposed volume change, the pressure relaxes only partially [69], [70], [71], [72], [73]. Once the steady creep stage is reached, the flow of a glass becomes isochoric, which is where Trouton's law [74] originates (see also [68]). Shear deformation and volumetric relaxation may exhibit different relaxation spectra [73]. This difference suggests that shear-driven rearrangements and pressure-induced volume-changing processes may involve partially distinct microscopic mechanisms, although they may still share some underlying structural features [75], but it remains unclear whether a universal link between these two processes exists across all glassy systems.

### 1.3 Physical origin of the delayed elasticity

Debye relaxation [76] refers to a relaxation process where the quantity of interest undergoes a single exponential decay. In the context of viscoelasticity, if the stress exhibits a pure exponential decay under constant strain, it indicates that the strain is simply the sum of elastic and viscous strains, with no delayed elasticity: this is the viscoelastic Maxwell model [77]. For glasses, viscous deformation is systematically accompanied by delayed elasticity, that is highlighted by the ”non-Debye” / ”non-Maxwellian” stress relaxation [3], [13], [39], [78] (interpreted early on as due to glass heterogeneities [79]), from room temperature [80], to high temperatures, slightly above their glass transition, where their delayed elasticity/non-exponentiality gradually vanishes [81]. Nonetheless, the universal mechanisms behind this strain component are still rather speculative.

It is now well established, for various amorphous systems, that shear transformations (STs) will induce a stress redistribution in their neighborhoods, as an inclusion bearing an eigenstrain (see [82] for the definition of eigen-strain/stress) does in the famous Eshelby’s problem [83]. This kind of mechanisms prevails even up to the glass transition range [84]. In terms of potential energy landscape (see [50]), when a macroscopical shear stress is applied, the group of atoms undergoing the shear transformation (the ”shear transformation zone”, hereafter STZ) overcomes an energy barrier, biased by this stress, to reach a new potential minima, with a new configuration/state. The issue raised by this picture was addressed by Orowan [85]: *”If the [macroscopical] stress is removed, the two potential energy minima of the initial and rearranged states are no longer biased. [...] In short, the deformation produced by the biasing influence of the stress on the relative energies of the two potential minima was not viscous flow at all, but a retarded elastic deformation”*. In other words, an individual ST does not produce any viscous flow, as the STZ keeps a memory of its initial state, towards which it tends to return, but it, therefore, produces only delayed elasticity.

This raises the question: ***How can delayed elasticity and viscous flow occur simultaneously, whereas their creation processes seem antagonistic?***

Orowan [85] solved this question by arguing that subsequent STs in the neighborhood would modify the stress in the first STZ, *”erase”* the *”memory”*, and thus makes it irreversible (see also [50]). This is, namely, using the words of Mazurin, a ”*memory erosion*” leading to a ”*forgetting effect*” [86]. This explanation is convenient to explain the origin of the irreversible viscous flow, but on the other side, the explanation for delayed elasticity is lost. An escape to this issue is proposed by Goldstein [50]: *”Each [new] rearrangement has a double effect: on the one hand it tends to incorporate irreversibly into the structure of the material the deformations associated with earlier rearrangements; on the other it too represents in part a recoverable strain, which must be converted to irrecoverable strain by rearrangements yet to take place.”* It implies that each STZ carries the memory associated with delayed elasticity only intermittently, before losing it to be re-created in its vicinity. However, a detailed explanation of the scale transition from this local, intermittent memory to the macroscopic delayed elasticity has never been provided.

### 1.4 Purpose of the model

On this basis, the present work proposes a model describing the viscoelastic response of glassy networks under shear stress, based solely on local and isolated shear transformations (STs), while disregarding other possible viscoelastic contributions. I assume that this shear transformation mechanism is universal in inorganic glasses. The

purpose of the present work is to show how delayed elasticity can arise from linear viscoelastic deformation within a shear-transformation framework. To this end, the model is reduced to its most fundamental ingredients.

## 2. A Model of Shear Transformation

### 2.1 General framework

The purpose of the model presented here is to simplify a ST-based model, such as those developed by Bulatov & Argon [87], Homer & Schuh [65], [88], or Van Loock [89], into its simplest form, capable of simulating linear delayed elasticity. During temperature changes, glasses are likely to undergo structural changes. Similarly, below the glass transition temperature, they can relax and modify their structure. I will only deal here with situations where glass remains ***isostructural***: this hypothesis is required to have identical kinetics of delayed elasticity creation and recovery during creep-recovery tests. As previously mentioned, during uniaxial creep or relaxation tests, glasses relax hydrostatic pressure, but only partially, so that the volume changes, but reversibly, after stress removal. This aspect is neglected here for simplicity: rearrangements are purely isochoric (pure shear transformations). Furthermore, the influence of the shear stress on the energy barrier of a ST depends on the hydrostatic pressure in metallic glasses [90]: for simplicity and because this dependence is not universal in all inorganic glasses, this effect is neglected here.

STs are thermally activated processes, biased by shear stress [91]. So, very basically, at low temperature (athermal conditions) they are driven by the stress field, whereas at high enough temperature they are also driven by the temperature. In this latter case, if the elastic potential energy provided by external stress is much lower than the energy barrier to overcome to produce a ST, and much lower than the thermal energy, the viscoelastic behavior is linear (none of the viscoelastic constants depend on stress or strain rate). I will restrict the study to the domain of linear viscoelasticity. Studies on the rheology of amorphous materials using ST-based mesoscale model exist in the literature [65], [87], [88], [89], [92], [93], but not in the domain of linear viscoelasticity, or with no focus on delayed elasticity, which, compared to plastic strain and viscous flow, has received little attention [94].

Whereas a ST corresponds to a local rearrangement of a group of atoms, it is assumed since a long time [50] that we don't need to describe each atomic motion to model the macroscopical strain they will induce. In a mesoscopical model, a STZ can be modeled as an inclusion undergoing an eigenstrain corresponding to a shear distortion $\gamma^p$, in the framework of continuum mechanics. Consequently, finite element analysis (FEA) can be used to model a sequence of STs [65], [87], [88], [89], [92], [93].

### 2.2 Linear viscoelasticity

Since STs are thermally activated processes, it means that in the glass transition domain, or above, even if no macroscopical stress is applied on the amorphous system, they continuously, randomly and spontaneously occur [49], [56], [95], [96]. The shear directions of STs are random, so that at no point do they induce macroscopic deformation: they basically compensate each other and/or go back and forth [56], [96]. And the other side, if a low macroscopical shear stress is added, STs are slightly biased [40], [56], [95], [97]. It does not necessarily mean that STs become stress-activated, but it means that the statistical distribution of shear directions of STs would be shifted

toward the direction of the macroscopical stress [56]: more STs occur in the direction of the applied stress and these are said to be *concordant* [50], [85] with this stress. To compensate, less STs occur in orthogonal directions (the *discordant* event). Nevertheless it could also be assumed that the overall frequency of STs increases with the stress. What is the contribution of both (increase of concordant/decrease of discordant STs and overall increase of ST frequency) will be clarified here.

Let us consider a 2D problem in plane stress, where $\sigma_{ij}$ is the stress tensor and $\epsilon_{ij}$ the strain tensor, expressed in the coordinate system $(x_1, x_2)$. A pure shear stress $\sigma_{12}$ is applied on a STZ. The STZ can undergo a ST where the distortion ($\gamma^p$) itself is not in the same direction: $\theta$ is the angle between the direction of the shear stress (of the maximal principal stress) and the one of the shear distortion. When $\theta = 0$, the ST is fully concordant with the stress (see Figure 1) and when $\theta = \pm\pi/2$ the ST is fully discordant (opposed to the shear stress). When $\theta = \pm\pi/4$ the ST is "neutral": neither concordant nor discordant.

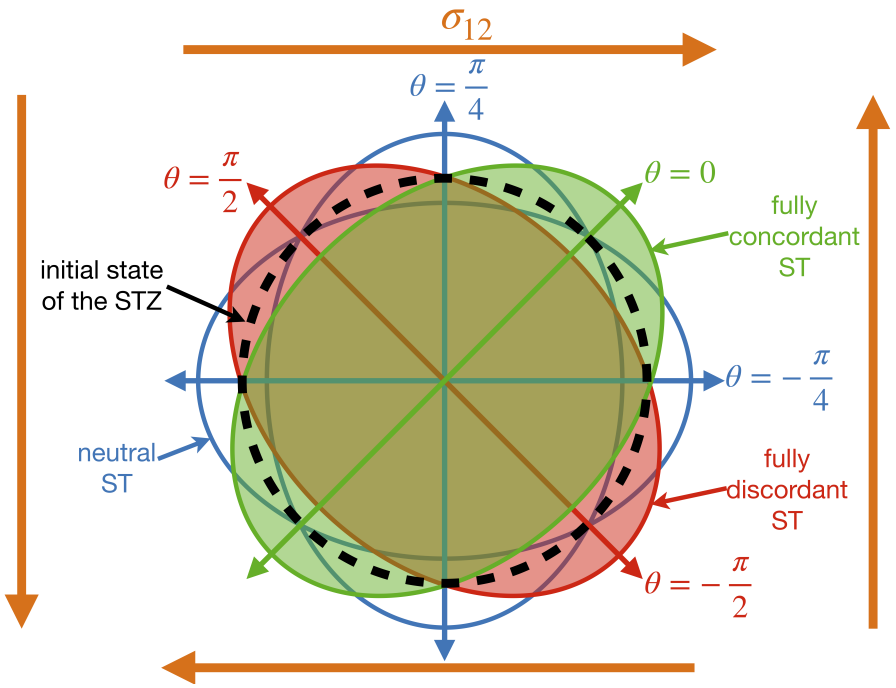


***Figure 1.*** *Schematic representation of STs, concordant, discordant and neutral, regarding the shear stress $\sigma_{12}$. $\mathbf{e}_1$ is the horizontal direction, $\mathbf{e}_2$ is the vertical one.*

From the transition state theory, the frequency (or activation rate) of a concordant event is given by [91]:

$$\dot{s}(\sigma_{12}) = f_0 \, e^{-\frac{\Delta G - \gamma^p \Omega \sigma_{12}}{kT}} \tag{1}$$

Where $\Delta G$ is the Gibbs energy for activation of the ST ("energy barrier"), and $\Omega$ the volume of the STZ, both possibly temperature dependent, but the investigations will be isothermal. Normalizing $\dot{s}$ so that the activation rate of a ST is 1 (adimensional unit) for $\sigma_{12} = 0$, the obtained adimensional activation rate is:

$$\dot{s}(\sigma_{12}) = e^{\frac{\gamma^p \Omega \sigma_{12}}{kT}} \tag{2}$$

where $\gamma^p \sim 0.1$ is a commonly accepted value for metallic glasses [4], [55], [91], [96]. From this equation, it is evident that the temperature range governs the extent of linear viscoelasticity: linear behavior is only observed when $T$ is high enough for $\dot{s}(\sigma_{12})$ to

be approximated as a linear function. As $T$ increases, the linear viscoelastic domain expands, extending to higher values of $\frac{\sigma_{12}}{\mu}$ (where $\mu$ is the shear elastic modulus). For oxide glasses, the linear viscoelastic domain corresponds to $\frac{\sigma_{12}}{\mu} < 10^{-3} - 10^{-2}$ [98], within the glass transition range. This behavior is similar in metallic glasses, where linear behavior is observed for $\frac{\sigma_{12}}{\mu} < 10^{-3}$ at the glass transition temperature ($T_g$), and extends to higher stresses as the temperature increases [65], [99]. Now $T$ needs to be defined, with adimensional values. $\gamma^p\Omega/kT$ unit is $m^3/J = Pa^{-1}$ so that:

$$\frac{\gamma^p\Omega}{kT} = \frac{a}{\mu} \tag{3}$$

where $a$ is an adimensional factor. Decreasing $a$ increase the temperature.

### 2.3 KMC algorithm

The method to simulate ST sequences is as follows [65], [88], [89]: at a given time step, as STZ is chosen and uniformly sheared in a given direction, one STZ at every time step. When a ST occurs, the stress induced in the neighborhood propagates from the STZ to the far field [100], [101]: it is assumed here that this stress field equilibrates before the next ST occurs in the region significantly impacted by this stress. Accordingly, the stress field resulting from a ST in its vicinity is calculated within the framework of linear elasticity, with (Einstein summation convention) $\sigma_{ij,j} = 0, \forall i$ (static stress field) [65], [88], [89]. A single STZ is chosen at every step $k$ using a kinetic Monte Carlo algorithm (KMC), as well as the time interval between two steps ($\Delta t_k$). The method used here is exactly the one described by Van Loock *et al.* [89], I will only described the detail that differs: the adimensional ST activation rates. To select a given STZ "$n$", among $N$ possible STZs, its probability and thus its activation rate $\dot{s}_n$ must be defined. In the adimensional investigation, I define as $\dot{s}_{0n}$ as the activation rate of transformation of the STZ $n$, without any stress applied. If the STZ $n$ undergoes a maximum shear stress $\tau_{max-n}$, that is not necessarily $\sigma_{12}$, $\dot{s}_n$ is given by (Eq.2 & Eq.3):

$$\dot{s}_n = \dot{s}_{0n}\, e^{\left(\frac{\gamma^p\Omega}{kT}\tau_{max-n}\right)} = \dot{s}_{0n}\, e^{a\,\frac{\tau_{max-n}}{\mu}} \tag{4}$$

and unless otherwise stated, $\dot{s}_{0n}$ is 1. Simulations will be discussed in terms of adimensional parameters $a$ fixing the temperature and $\sigma_{12}/\mu$ fixing the macroscopical stress level.

### 2.4 Finite Element Analysis

Once every $\dot{s}_n$ has been calculated at the end of the step $k-1$, a single STZ is selected by the KMC algorithm, among the $N$ possible STZs, for the new transformation of the step $k$. Since the problem of this transformation can be treated using continuum mechanics, it is solved by the finite element method, here using the Cast3M software [102]. The problem is solved using exactly, step by step, the Eshelby's method (see also the Fig.1 of [103] for the step-by-step diagram of this method), using a "*sequence of imaginary cutting, straining and welding operations*" [83], an STZ being an Eshelby's inclusion. A single STZ $n$ is transformed per step time, and its transformation (the "eigenstrain") is imposed as a homogeneous inelastic pure shear distortion $\gamma^p = 0.1$, in the direction of its maximal shear stress $\tau_{max-n}$ (average value across the STZ $n$), as defined by the Mohr's circle (see Van Loock *et al.* [89]).

The elastic moduli are homogenous all over the mesh for simplicity, but this should have little qualitative effect on results [92]. For simplicity, the bulk modulus is taken as $k \to +\infty$, assuming incompressible strain. This choice reduces model complexity and fixes a parameter. The problem is solved in 2D plane stress ($\sigma_{i3} = 0$, $\forall i$, corresponding to a thin geometry) under the small strain assumption. Indeed, combining plane strain conditions with incompressibility would lead to overly constrained deformation fields ($\epsilon_{11} = -\epsilon_{22}$), while the associated stress field $\sigma_{12}$ would remain localized within the STZ, with no long-range elastic interactions. Periodic boundary conditions are applied. The system is made of a square mesh, having an adimensional size of $1 \times 1$ in the $(\mathbf{e}_1, \mathbf{e}_2)$ plane, and a STZ corresponds to a part of this mesh made of some neighboring elements. The mechanical loading investigated here is constant shear stress, namely creep/recovery (the stress is null for recovery).

When $\gamma^p_{12}$, $\epsilon^p_{12}$ ($\epsilon^p_{ij} = \gamma^p_{ij}/2$) or $\sigma_{12}$ are given, it corresponds to the average values across the mesh, $\gamma^p_{12}(x_1, x_2)$, $\epsilon^p_{12}(x_1, x_2)$ or $\sigma_{12}(x_1, x_2)$ refer to local values within the mesh. $x_1$ is the horizontal coordinate, $x_2$ the vertical coordinate. $x_1 = 0$ and $x_2 = 0$ correspond to the center of the mesh.

## 2.5 Rheological models

### 2.5.1 Maxwell fluid

The Maxwell fluid corresponds to a rheological model exhibiting no delayed elasticity [77], [78]. To my knowledge, no glass shows such behavior in its glass transition range. The purpose here is to try to develop such model, to highlight that obtaining viscous deformation without delayed elasticity is complex, a key to understand why no glass shows this behavior. The special feature of the Maxwell's model is that it has only one relaxation time. This relaxation time is related to the activation rate of transformation events [3], [104]. That is to say, all STs are strictly identical. In order to satisfy this criterion, one has to avoid any STZs superposition, creating domain intersections with high apparent activation rates. Additionally, all STZs must have the same properties, and consequently the same shape/size. One easy way to achieve this situation is to use quadrilateral elements. The system is thus meshed by 10000 square elements, all identical, with 4 nodes. A STZ consists of 4 elements sharing the same node, so that the system is made of 2500 strictly identical STZs, with $\dot{s}_{0n} = 1, \ \forall n$. The shape and the number of element per STZ sounds maybe "unrealistic", but I agree with Goldstein [50] that "*the changes in atomic positions in the [STZ] do not even approximately resemble displacements we might calculate from phenomenological elasticity*" and "*may be replaced by [...] whatever happens to be convenient*" to produce the long-range stress field around the STZ, the keystone of the qualitative results I will discuss here. Additionally, Sandfeld *et al.* [105] showed that using a relatively coarse quadratic mesh has only a limited impact on the stress field near the STZ, and they emphasized that an STZ cannot be characterized by a single, well-defined geometry (for molecular dynamics images of STZs and their shapes, see Zhen *et al.* [106]). However, the square geometry of the STZ introduces an anisotropy, which will be discussed later. The purpose of mesh refinement is to obtain a finite-element solution that matches that of continuum mechanics (the Eshelby's problem). However, an STZ comprises at most a few tens of atoms, which is far smaller than the scale of a representative volume element. Consequently, further refinement cannot guarantee convergence to the actual solution, as Goldstein statement implies.

### 2.5.2 Viscoelastic solid

Viscoelastic solids are usually defined as viscoelastic bodies exhibiting delayed elasticity without viscous flow [107]. In this respect, a viscoelastic solid is the exact opposite of a Maxwell fluid. The simplest rheological model of a viscoelastic solid is the standard linear solid [41], [43], [108]. The purpose here is to obtain such behavior, starting from the Maxwell model previously described, by minimizing the modifications, to ensure that -additional- delayed elasticity is only the result of these small changes. So I just select randomly 1000 STZs of the Maxwell model, that become the only ones active STZs. All other parameters of the model (STZ shape, method... and $\dot{s}_{0n} = 1$ for all active STZs) stay the same. The map of active STZs is shown on Figure 2.

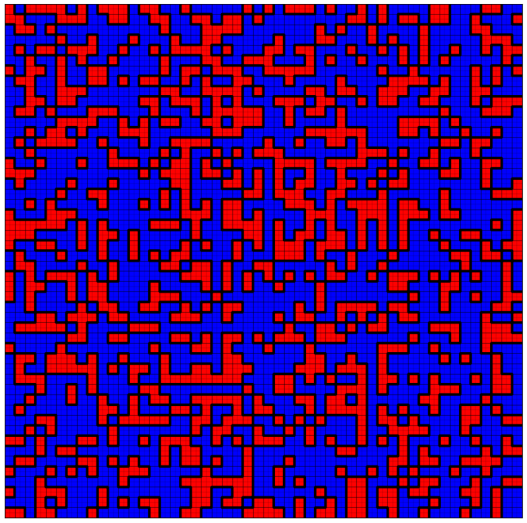

***Figure 2.*** *Map of slow (blue) and fast (red) STZs for the viscoelastic fluid model (respectively: inactive and active domains for the viscoelastic solid model). The grid is the mesh.*

### 2.5.3 Viscoelastic fluid

Viscoelastic fluids are usually defined as viscoelastic bodies exhibiting delayed elasticity and viscous flow [107]. In order to create a viscoelastic fluid, the model must have a distribution of relaxation times [13] (distribution of STZ activation rates). The purpose here is to obtain such behavior, starting from the Maxwell model previously described, by minimizing the modifications, to ensure that -additional- delayed elasticity is only the result of these small changes. So I just select randomly 1000 STZs of the Maxwell model, and keep $\dot{s}_{0n} = 1$ for these STZs (namely: "*fast STZ*"), the other 1500 STZs (namely: "*slow STZ*") are now defined by $\dot{s}_{0n} = 0.01$: see Figure 2. Thus, the ingredient added is a distribution of activation rates without any distribution of stress sensitivity or eigenstrain ($\gamma^p$).

# 3. Results

## 3.1 Maxwell model

### 3.1.1 Simulation temperature selection

In order to extend the domain of linear viscoelasticity (the domain where $kT > \gamma^p \Omega \sigma_{12}$) up to at least $\sim 10^{-3}$, it is necessary that $a$ be less than 500 (see Eq.4). In the case of low values of $\sigma_{12}/\mu$ ($<< \gamma^p$), when a ST occurs, the activation rate $\dot{s}_n$ inside the corresponding STZ increases. This will be discussed in more detail later on. As a result, this STZ is the optimal candidate for the next transformation. The higher the temperature at given $\sigma_{12}/\mu$, the smaller the increase of $\dot{s}_n$ in the STZ. First simulations show that, at $\sigma_{12}/\mu \leq 10^{-3}$, if the temperature is too low ($a \geq 250$), STZs just go back and forth: In most cases, if a ST occurs at a given time step, it will revert to its initial configuration at the next step. The deformation rate during creep is consequently very low and very noisy. To extend the lifetime of a STZ in their transformed state, it is necessary to reduce the value of $a$ to 150. With this value, $\sim 0.5\%$ of STZs immediately transform back (the lifetime of a STZ between two successive transformations is larger than 100 steps).

For the sake of order-of-magnitude estimates only, with $\Omega = 0.8\ nm^3$ for Vitreloy 1 [65], taking into account the decay of $\mu$ is this temperature region: $a = 150$ would typically correspond for this glass to 1.2 to 1.4 $T_g$ (K) (Eq.3).

### 3.1.2 Dynamic Equilibrium

The mesh is initially free of any stress, and it sounds easy to consider this state as the ”reference state”, and to start creep simulations from this state. It is known that in this situation the viscoelastic behavior is not stable, since the system is not equilibrated [65]: the creep rate decays rapidly and unexpectedly after several thousand steps (simulation not shown). Actually, such a stress-free state has no reason to exist in a glass [57], [65], [109]. When the first ST occurs, the corresponding STZ is not selected at the next step, at $a = 150$: many STs occur before the first STZ is selected again. Consequently, the stress becomes heterogenous, and it is unlikely that a sequence of STs will cause a return to the state of zero stress. In order to create a (dynamically) stable initial stress-state for further simulations, a first simulation is made with the Maxwell model with no stress applied. A random STZ is selected for the first step of the simulation, transformed, and then the system is left free of macroscopical stress during 67 000 steps ($t \sim 6.8$). The system is considered stable because neither the standard deviation of $\sigma_{12}(x_1, x_2)$ nor the total activation rate ($\dot{s}_{tot} = \sum_N \dot{s}_n$) evolves: see Figure 3. At first, as there is no stress applied, $\dot{s}_{tot} = \sum_{2500} \dot{s}_{0n} = 2500$. Then, due to STs, the stress becomes heterogeneous, $\tau_{max}$ increases in every STZ, and thus $\dot{s}_{tot}$ increases before decaying and stabilizing at $\dot{s}_{tot} \sim 9000$.

This final state ($t \sim 6.8$) is stable but dynamic: its statistical parameters are stable, but the stress field permanently fluctuates. Consequently, the creep-recovery tests will be started from this state, considered as the reference state. In the following simulations, $t = 0$ corresponds to the reference state, and the $\gamma^p_{12}(x_1, x_2)$ field shown for the following simulations correspond to the actual $\gamma^p_{12}(x_1, x_2)$ field minus the $\gamma^p_{12}(x_1, x_2)$ field of the reference state.

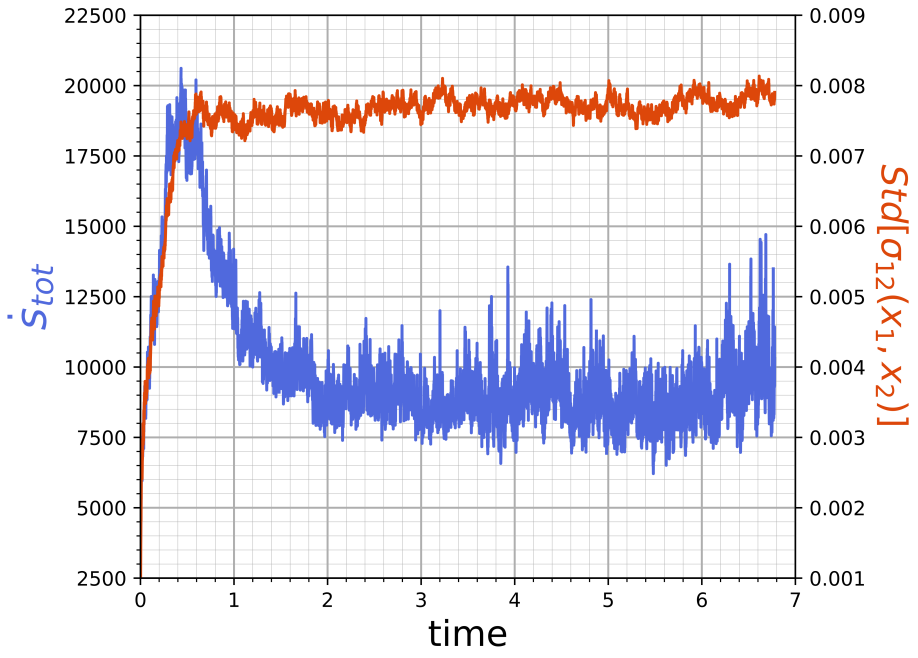


***Figure 3.*** *Evolution of the total activation rate ($\dot{s}_{tot}$, left, blue) and the standard deviation of $\sigma_{12}(x_1, x_2)$ ($Std[\sigma_{12}(x_1, x_2)]$, right, red) of the Maxwell model under no macroscopical stress. The time has no unit: it is relative to the inverse of the activation rate of a stress-free STZ ($\dot{s}_{0n}^{-1}$).*

### 3.1.3 Boundary of Linear Viscoelastic Domain

By definition, the linear domain is the stress domain where creep compliance ($\gamma_{12}(t)/\sigma_{12}$) is independent of stress. Consequently, the $\gamma_{12}^{p}(t)/(\sigma_{12}/\mu)$ curves superimpose in this domain (Fig.4). The limit of linear viscoelasticity ("newtonian region") is somewhere between $\sigma_{12}/\mu = 2.10^{-3}$ and $\sigma_{12}/\mu = 10^{-2}$ at the temperature investigated here, which is consistent with the simulation of Homer *et al.* [65]. At $\sigma_{12}/\mu = 4.10^{-3}$, we can already see a slight deviation from linearity.

For all stresses in the linear domain, $\dot{s}_{tot}$ is close to $\sim 9000$ (Fig.5), but fluctuates widely over time (as during the stabilization for $t \geq 3$: Fig.3), with a standard deviation around $\sim 1000$. It is rather stress insensitive. From Eq.2, as a rough estimate, if all STZs support a stress of $\sigma_{12}/\mu = 2.10^{-3}$, $\dot{s}_{tot}$ would increase by $\sim 875$, compared to $\sigma_{12}/\mu = 0$, a value less than the fluctuation of $\dot{s}_{tot}$ (see the blue curve on Fig.5). Similarly, the standard deviation of $\sigma_{12}(x_1, x_2)/\mu$ is stable ($0.0079 \pm 0.0002$) [3] whatever the stress. Conversely, the ratio of concordant ($\mid \theta \mid < 45°$, see Fig.1) to discordant ($\mid \theta \mid > 45°$) event rates ($r_{c/d}$) increases in proportion to the stress (Fig.5). In the linear domain, STs are mostly thermally activated, and not stress-activated: they exhibiting no change in their overall activation rate in response to stress, because this rate is mainly due to random thermally activated events. The observed increase in creep rate can be attributed to an increase in concordant event rates and a reduction in discordant event rates: the distribution of events is biased. These two variations offset each other, maintaining a constant overall event rate. This, in turn, gives rise to a linear viscoelastic behavior.

[3] Model-wide stress standard deviations are computed over all nodes; thereafter, stress standard deviations reported for STZs are computed using only the stress at the central node, excluding peripheral STZ nodes from the calculation.

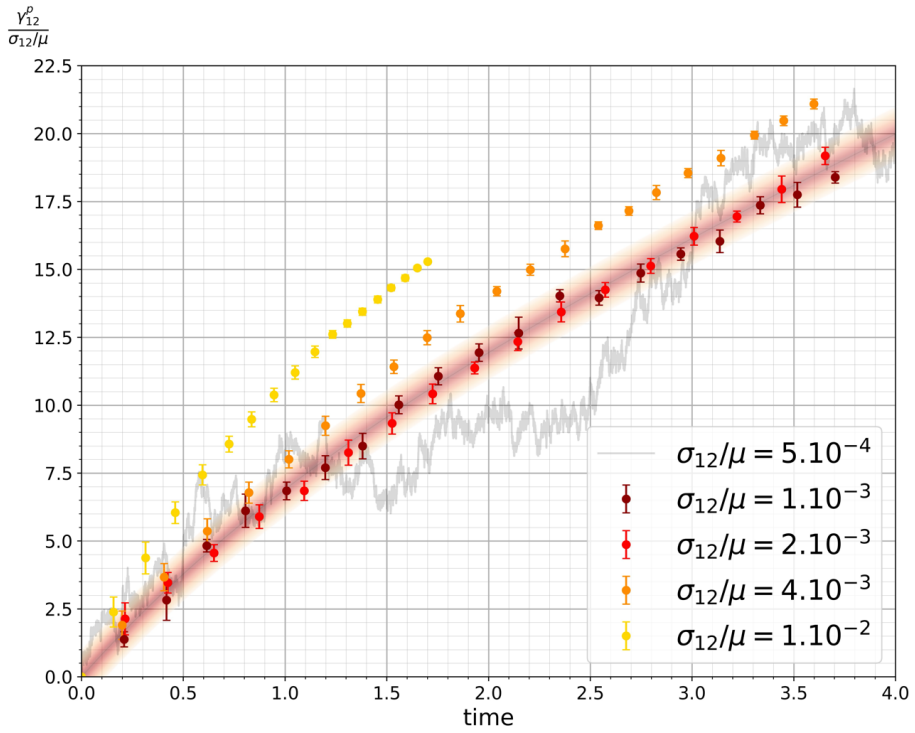


***Figure 4.*** *Normalized inelastic strain ($\gamma^p_{12}(t)/(\sigma_{12}/\mu)$) vs. time for the Maxwell model during creep, for various stress applied. The colored strip highlights the linear domain. The data at $\sigma_{12}/\mu = 5.10^{-4}$, which are rather noisy, are plotted with some transparency for clarity.*

It must be noted that with no macroscopical stress, the system is in a dynamic equilibrium, where STs are driven by a heterogenous stress field $\sigma_{12}(x_1, x_2)/\mu$ with a quite large standard deviation ($\sim 8.10^{-3}$). If a macroscopical stress is added, within the linear viscoelastic domain ($\sigma_{12}/\mu < 4.10^{-3}$), this stress is much smaller than the average stress fluctuation supported by the STZs: the macroscopical stress can only slightly bias the dynamic of STs, and this is the reason why $\dot{s}_{tot}$ is not impacted by the stress.

On the other side, if we leave the linear domain $\dot{s}_{tot}$, the standard deviation of $\sigma_{12}(x_1, x_2)$ both increase continuously over time, whereas $r_{c/d}$ decreases continuously. The simulation was not run long enough to see if they tend to stabilize: the nonlinear domain is not the subject of this study. At $\sigma_{12}/\mu = 4.10^{-3}$ we can see signatures of non-linearity: the standard deviation of $\sigma_{12}(x_1, x_2)$ slightly increases over times and $r_{c/d}$ are not stable all over the simulation. Indeed, $r_{c/d} \sim 1.2$ for the first 10 000 steps and ends at $r_{c/d} \sim 1.09$ for the last 10 000 steps.

To ensure that the simulation results are within the linear viscoelastic domain, further simulations will be performed at a shear stress ratio of $\sigma_{12}/\mu \leq 2.10^{-3}$.

### 3.1.4 Creep-recovery

A creep-recovery test is performed after equilibration. The creep test ($\sigma_{12}/\mu = 10^{-3}$) stops at the step $50000$ ($t = 4.91$), to start the recovery ($\sigma_{12}/\mu = 0$). The result is shown on Fig.6. $\gamma^p_{12}$ does not linearly evolve over time during creep, as expected for a Maxwell model, instead, the creep compliance is the one of a Burger's model [110]:

$$J(t) = \frac{1}{\mu} + \frac{1}{\mu_d}\left(1 - \exp\left(-\frac{t}{\tau_d}\right)\right) + \frac{t}{\eta} \tag{5}$$

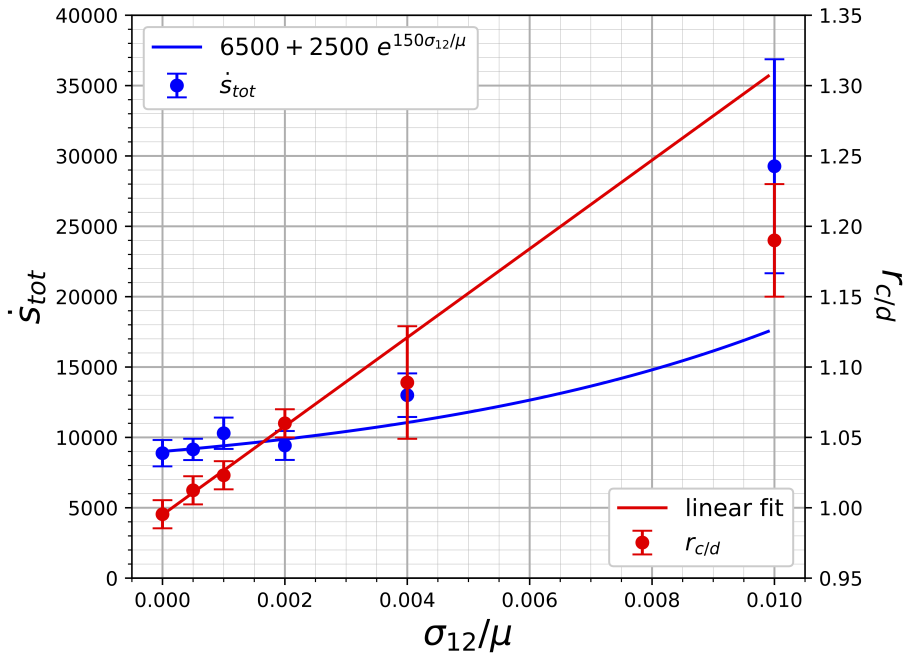


***Figure 5.*** *Evolution of the total activation rate ($\dot{s}_{tot}$) and the ratio of concordant ($\mid \theta \mid < 45°$, see Fig.1) to discordant ($\mid \theta \mid > 45°$) event rates ($r_{c/d}$) as a function of the normalized stress $\sigma_{12}/\mu$ for the Maxwell model. The values are stable all over the simulation for $\sigma_{12}/\mu \leq 2.10^{-3}$, and error bars are the standard deviations. For $\sigma_{12}/\mu \geq 4.10^{-3}$, the values are calculated for the last half of the simulations, since they continuously evolve.*

with $\mu_d = \mu/4.6$, $\eta = \mu/3.6$ and $\tau_d = 1/2$. In summary, a portion of the non-elastic strain is attributable to delayed elasticity, which undergoes a recovery. The other component of non-elastic strain is viscous strain, which, on average, increases during creep at a rate of $\sim \gamma^p/(114N)$ per time step ($N$ is the number of STZ). This indicates that it is $114$ times slower than if all ST were perfectly concordant.

During the whole simulation, the standard deviation of $\sigma_{12}(x_1, x_2)$ is stable ($0.0079 \pm 0.0001$) as well as $\dot{s}_{tot}$ ($10^4 \pm 10^3$). The stress distribution is Gaussian throughout the simulation, but centered at $\sigma_{12}/\mu = 10^{-3}$ during creep and at 0 during recovery. On the other side, if $r_{c/d}$ is quite stable during creep ($1.02$), at the beginning of recovery ($4.91 < t < 5.94$: 10000 steps) it decays down to $0.97$ and then increases to stabilize at $r_{c/d} = 1.00$ at the end of recovery. The creep is thus due to an excess of concordant events, the partial recovery to an excess of discordant events (regarding the stress applied during creep), and a rebalancing of the ratio of concordant to discordant events occurs as recovery progresses. At the final stage of creep, there are 1.16 times more domain supporting positive $\sigma_{12}$ than negative, whereas at the end of recovery, the ratio is 1.00, in agreement with the $r_{c/d}$ ratios.

The inelastic strain maps during creep are shown on Fig.7. At the onset of creep, the inelastic strain $\gamma^p_{12}$ is distinctly localized into two bands (one in the middle and one at the top-bottom crossing the periodic boundary). However, $\gamma^p_{12}$ rapidly homogenizes, but in these two bands $\mid \gamma^p_{12} \mid$ remains larger. Interestingly, many STZs undergo STs, but stay at a low level of $\gamma^p_{12}$ (white domains on Fig.7): they undergo mainly neutral STs or/and they go "back and forth" and cancel their inelastic strain between two successive STs. Similarly, at the end of creep, the maximum local inelastic strain is $\gamma^p_{12}(x_1, x_2)/\gamma^p = 4$, whereas some STs have occurred up to 100 times, underlying, as the slow viscous strain rate does, the inefficiency of STZs to accumulate inelastic strain.

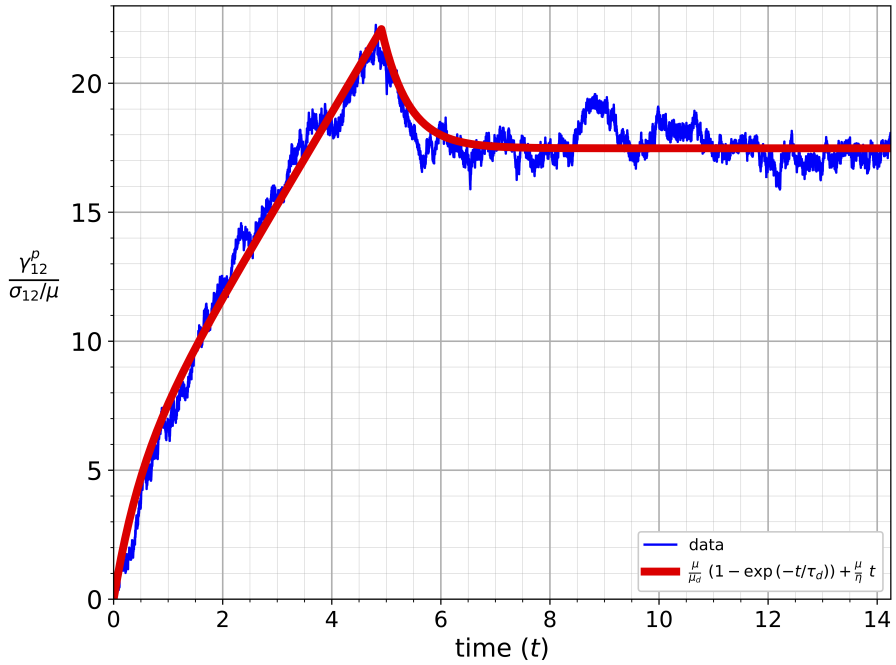


***Figure 6. Maxwell model.*** *Normalized inelastic strain ($\gamma^p_{12}(t)/(\sigma_{12}/\mu)$, where $\sigma_{12}$ is the stress applied during creep) vs. time for the Maxwell model during creep ($t \leq 4.91$) and recovery ($t > 4.91$) and its best fit using the creep compliance of Eq.(5).*

Comparably, when the recovery starts (Fig.8), the STZs in the same two bands are first activated, the majority of them to recover their inelastic strain ($\sim 55\%$ of them at $t = 5.38$), and as time progresses, the new STs are more homogeneously distributed, and the ratio of STs recovering inelastic strain to the STs creating new inelastic strain equilibrates.

The distribution of inelastic strain (Fig.9) is not Gaussian. At the end of creep, a very large fraction of STZs have virtually no inelastic strain, and the distribution is clearly shifted to the right (positive $\gamma^p_{12}$), with some excess of elements having $\gamma^p_{12} \sim \gamma^p$. At the end of recovery, the fraction of STZs having significant inelastic strain increases, the distribution shifts to the left (negative $\gamma^p_{12}$), with a significant increase of STZs with $\gamma^p_{12} < -\gamma^p$, and a significant decrease of STZs with $\gamma^p_{12} \sim \gamma^p$, suggesting that these latter STZs drastically tend to recover their inelastic strain.

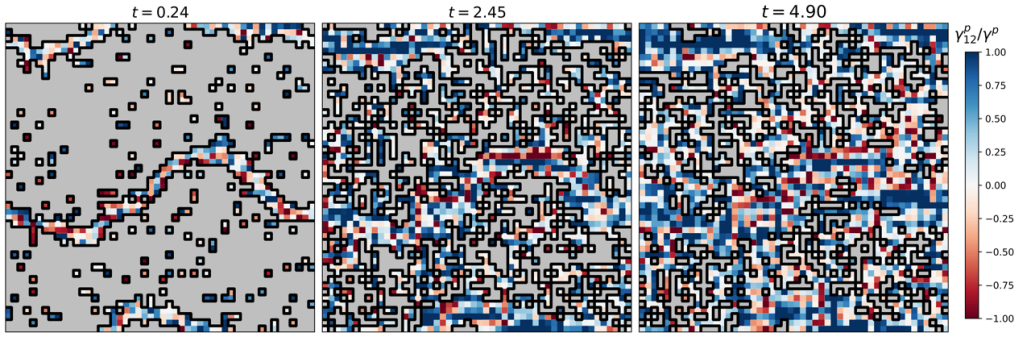


***Figure 7. Maxwell model.*** *Inelastic strain map ($\gamma^p_{12}(x_1, x_2, t)$) normalized by the inelastic distortion of a ST ($\gamma^p$) during creep at various step time. The black lines delineate the boundary between the gray domains where no ST has ever occurred since the beginning of creep and those where STs have occurred. $\gamma^p_{12}(x_1, x_2, t)$ is calculated from the reference state ($t = 0$).*

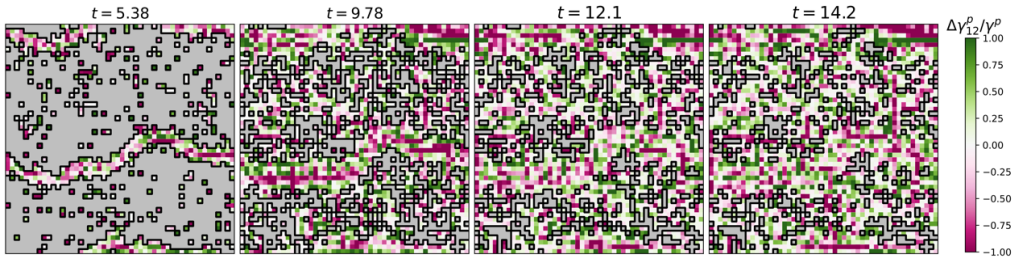


***Figure 8. Maxwell model.*** *Inelastic strain map change during recovery ($\Delta\gamma^p_{12}(x_1,x_2,t) = \gamma^p_{12}(x_1,x_2,t) - \gamma^p_{12}(x_1,x_2,t=4.91)$) normalized by the distortion of a ST ($\gamma^p$) at various step time. Pink domains recovers a part of their inelastic strain, green domains create more inelastic strain. The black lines delineate the boundary between the gray domains where no ST has ever occurred since the beginning of the recovery ($t = 4.91$) and those where STs have occurred.*

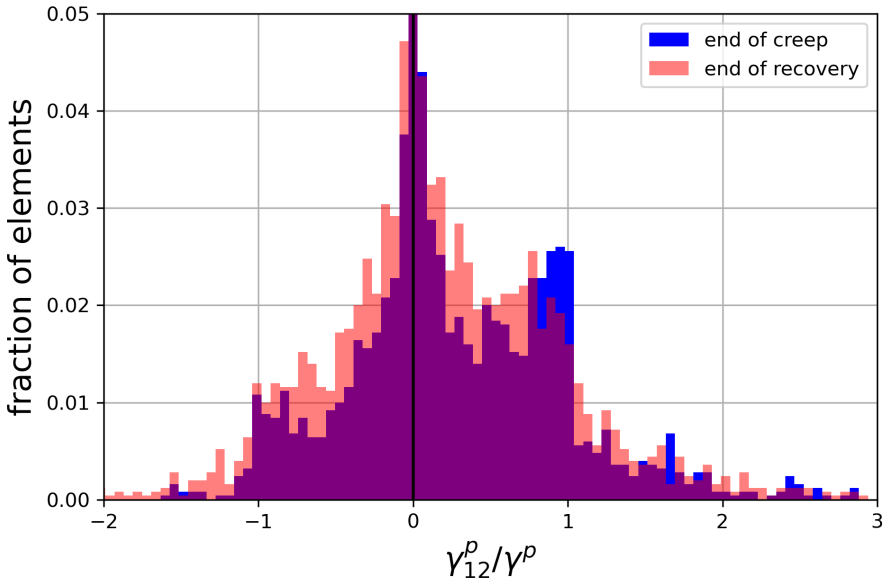


***Figure 9. Maxwell model.*** *Histogram of inelastic strain ($\gamma^p_{12}/\gamma^p$) at the end of creep and at the end of recovery.*

At the end of creep, the average inelastic strain is $\gamma^p_{12}(t = 4.90) \sim 0.220\gamma^p$, and recovers down to $\gamma^p_{12}(t = 14.2) \sim 0.174\gamma^p$, so that the recovery is $\sim 0.046\gamma^p$ (see Fig.6). At the end of creep there is 1.77 times more domains with $\gamma^p_{12} > 0$ than with $\gamma^p_{12} < 0$. At the end of recovery, the ratio is 1.39. In the domains where $\gamma^p_{12}(x_1, x_2, t = 4.90)$ is larger than $0.21\gamma^p$ (deep blue domain in Fig.7), the average recovery is $\sim 0.079\gamma^p$. That is, these domains recover much more than the others, and some of these other domains actually create additional inelastic strain instead of recovering it. The delayed elastic deformation that occurs for this "Maxwell model" is due to the formation of these two initial bands where excess inelastic strain is generated during creep and then recovered once the macroscopic stress is removed. The memory of the glass seems to be spatially localized in these bands and rather permanently, not intermittently.

### 3.2 Viscoelastic solid

As for the Maxwell model, the system is first equilibrated, without macroscopical stress, here during 138000 steps in order to reach a stable $\dot{s}_{tot}$ $(7970 \pm 246)$ and a stable standard deviation of $\sigma_{12}(x_1, x_2)/\mu$ $(0.0058 \pm 0.0001)$. Only STZs produce inelastic strain and have the ability to modify their stress by their own. However, their transformations

generate a long-range stress field, thereby causing the elastic and inactive domains to exhibit fluctuating stress, even those not in direct contact with a STZ.

I ran creep and creep recovery tests with $\sigma_{12}/\mu = 2.10^{-3}$ for creep. The result is shown on Fig.10. The stress applied remained within the linear viscoelastic domain, as evidenced by the stability of $\dot{s}_{tot}$ $(7980 \pm 361)$.

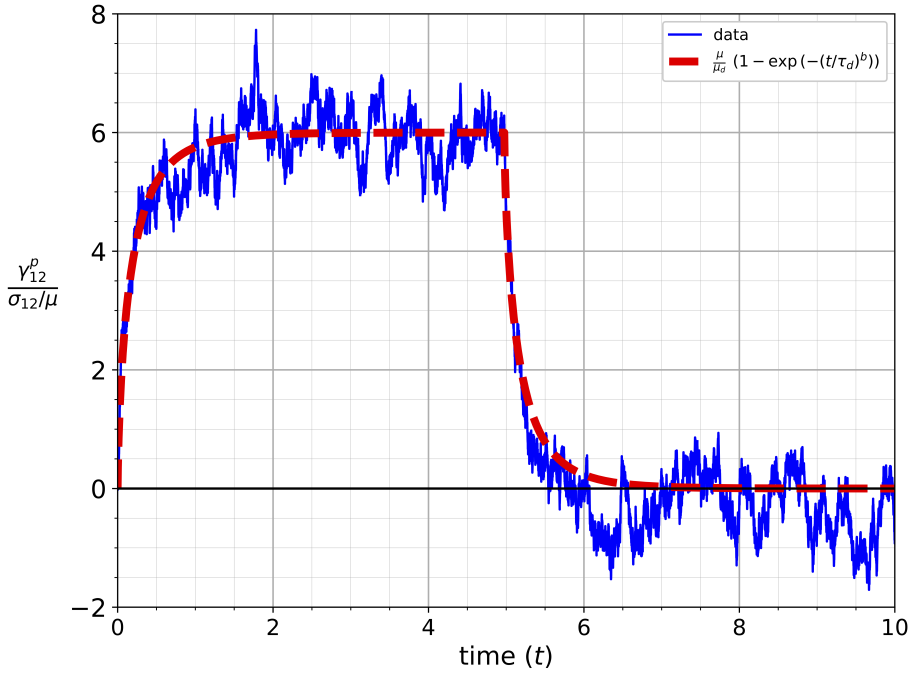


***Figure 10. Viscoelastic solid.*** *Normalized inelastic strain ($\gamma^p_{12}(t)/(\sigma_{12}/\mu)$, where $\sigma_{12}$ is the stress applied during creep) vs. time for the viscoelastic solid model during creep ($t \leq 4.97$) and recovery ($t > 4.97$) and its best fit. The recovery was run up to $t = 25$ (190 000 steps), and $\gamma^p_{12}(t)$ stays close to 0.*

As expected for a viscoelastic solid, $\gamma^p_{12}(t)$ increases during creep and then reaches a plateau. The creep compliance is:

$$J(t) = \frac{1}{\mu} + \frac{1}{\mu_d}\left(1 - \exp\left(-\left(\frac{t}{\tau_d}\right)^b\right)\right) \tag{6}$$

with $\mu_d = \mu/6.0$, $b = 0.7$ and $\tau_d = 0.19$. As for the Maxwell model, this stress applied for creep is much smaller than the average stress fluctuation supported by the STZs: the stress applied just slightly biases the dynamic of STs. As seen on Fig. 11, as soon as creep starts the average stress supported by the STZs decreases, and in return the average stress supported by the elastic inactive domains increases. Both categories show a Gaussian distribution of stresses, with statistical characteristics shown on Fig. 11.

The distribution of inelastic strain is shown on Fig.12. At the end of creep, not all STZs have positive inelastic strain, most of STZs have accumulated almost no inelastic strain, but the distribution is clearly shifted to the right ($\gamma^p_{12} > 0$). During recovery, the distribution shifts to the left and centers at $\gamma^p_{12} = 0$.

### 3.3 Viscoelastic fluid

Again, the system is first equilibrated, without macroscopical stress, here during 1 047 000 steps in order to reach a rather stable $\dot{s}_{tot}$ $(4835 \pm 576)$ and a stable standard

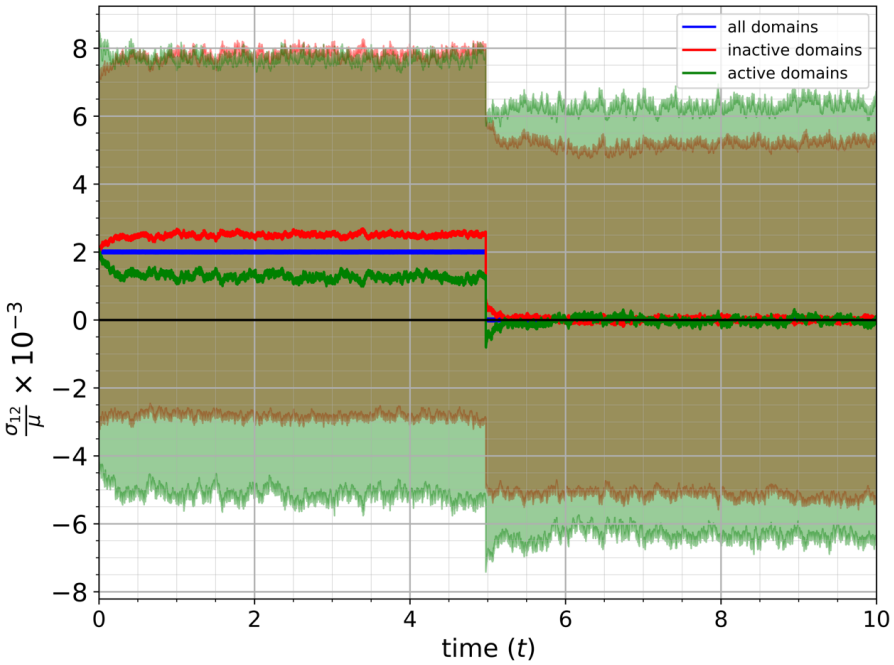


***Figure 11. Viscoelastic solid.*** *Average stress in the different domains of the viscoelastic solid (full lines): the active domains (STZ), the inactive domains (purely elastic), and in all domains. The colored filled areas of the graph represent the standard deviation (computed on the element field).*

deviation of $\sigma_{12}(x_1, x_2)/\mu$ $(0.0078 \pm 0.0001)$, with qualitatively the same evolutions as for the Maxwell model (Fig.3). At the first time step, when the system is free of stress, a fast ST is $\sim 66.7$ times more likely to occur than a slow ST, considering the number of each type of STZs and their respective activation rates. During the stabilization process, the occurrence of fast STZs stabilizes at $79 \pm 27$ times the occurrence of slow STZs (rolling average on last 100000 steps).

I ran creep (250000 steps) and recovery tests with $\sigma_{12}/\mu = 2.10^{-3}$ for creep. $\dot{s}_{tot}$ mays decrease but not significantly $(4211 \pm 656)$ and the standard deviation of $\sigma_{12}(x_1, x_2)/\mu$ $(0.0079 \pm 0.0002)$ stays stable, indicating that the stress applied falls within the linear viscoelastic domain. The result is shown on Fig.13. The creep–recovery curve is best fitted using the following creep compliance:

$$J(t) = \frac{1}{\mu} + \frac{1}{\mu_d}\left(1 - \exp\left(-\left(\frac{t}{\tau_d}\right)^{1/2}\right)\right) + \frac{t}{\eta} \tag{7}$$

With $\eta = 8\mu,\ \tau_d = 12.45,\ \mu_d = \mu/5.1$. At first glance, it may appear that two shear bands emerge at the very onset of creep (see Fig. 14). However, since inelastic strain initially develops in fast domains, these apparent bands are more likely regions separated by slow STZs rather than true shear bands. By the end of the creep phase, $99.8\%$ of fast STZs have undergone inelastic strain, compared to only $62.5\%$ of slow STZs.

As expected, fast STZs initially produce inelastic strain at a higher rate. However, they support less and less stress over time, which is transferred back to slow STZs (Fig.16). This stress transfer is similar to what is observed for the viscoelastic solid (Fig.11). Consequently, the strain rate of the fast domains quickly decreases, approaching that of the slow domains (Fig.13), otherwise, the stress level would increase in the fast domains. In other words, the fast domains relax their stress to nearly zero at the expense of the slow domains by maintaining a higher creep rate.

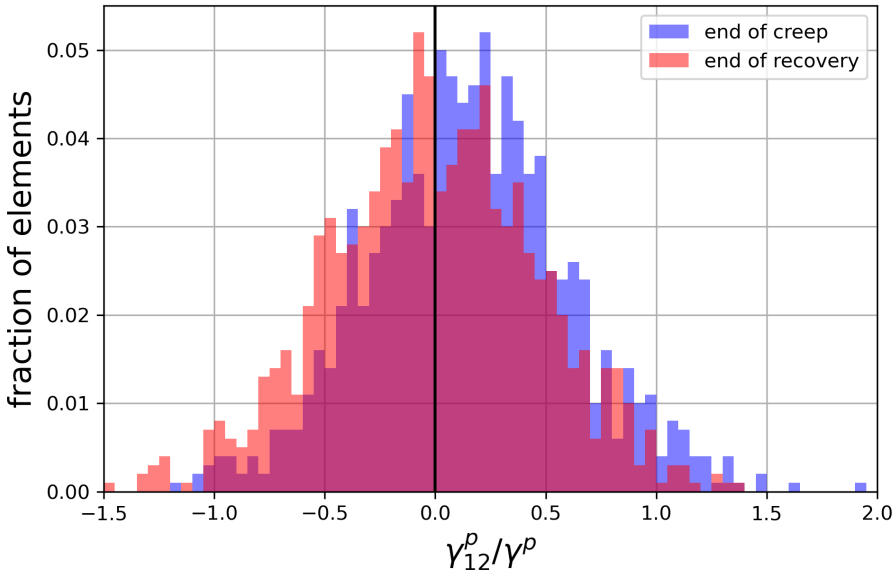


***Figure 12. Viscoelastic solid.*** *Histogram of inelastic strain ( $\gamma^p_{12}/\gamma^p$) at the end of creep ($t = 4.97$) and at the end of recovery ($t = 25$): fraction of elements among those having inelastic strain (elements having strictly no inelastic strain are excluded from the histogram; consequently inherently inactive elements are excluded) vs. normalized inelastic strain.*

Slow STZs have an insignificant contribution to recovery as illustrated on Fig.13. They are active (Fig.15), but in an inefficient way to promote recovery or additional inelastic strain. Consequently, I will focus on fast STZ.

Fig.17 shows that, at the onset of recovery, a large portion of fast STZs $(35.4\%)$ that have accumulated significant inelastic strain -upper part- experience negative -left part -stress (*i.e.*, back stress), and *vice versa*. All STZs exhibiting significant inelastic strain (greater than $\gamma^p$) recover (shown in pink), but they constitute only a small fraction of the fast STZs $(9.7\%)$. The relationship between the excess inelastic strain, the back stress at the onset of recovery, and the tendency to recover is very weak. The large number of STZs on the right side of Fig.17 (under positive stress) that eventually recover (shown in pink) highlights this weak correlation between back stress at the onset of recovery and amplitude of recovery. Furthermore, no continuous recovery of fast STZs is observed, even when the recovery begins from a state with a large excess of inelastic strain (Fig.18). In other words, the ”memory” driving recovery is not local but collective: fast STZ tend to recover together because, on average, they experience a negative stress, which is drowned in the random stress fluctuation.

## 4. Discussion

### 4.1 Shear transformations in the framework on linear viscoelasticity

A ST corresponds to the problem of Eshelby's spherical inclusion [83], for which an analytical solution exists. In this case, the inclusion undergoes a pure shear deformation ($\gamma^p$) as an eigenstrain. Let us assume that before the transformation the full system (the spherical inclusion and the surroundings) undergoes an homogeneous pure shear distortion $\sigma_{12}/\mu > 0$. If $\gamma^p >> \sigma_{12}/\mu$, after its transformation, a STZ will support a negative shear stress $\sigma^{STZ}_{12}$, called ”*back stress*” [49]. If $\sigma_{12}/\mu = \gamma^p/100$, $\sigma^{STZ}_{12}/\mu \sim -0.08$ (if the Poisson's ratio is 0.5) [83], [111]. Thus, if $\gamma^p = 0.1$ and $\sigma_{12}/\mu = 0.001$, the amplitude of $\sigma^{STZ}_{12}$ is 80 larger than $\sigma_{12}$. $\sigma^{STZ}_{12}$ tends to 0 when $\sigma_{12}/\mu = 0.8\gamma^p$ and then becomes

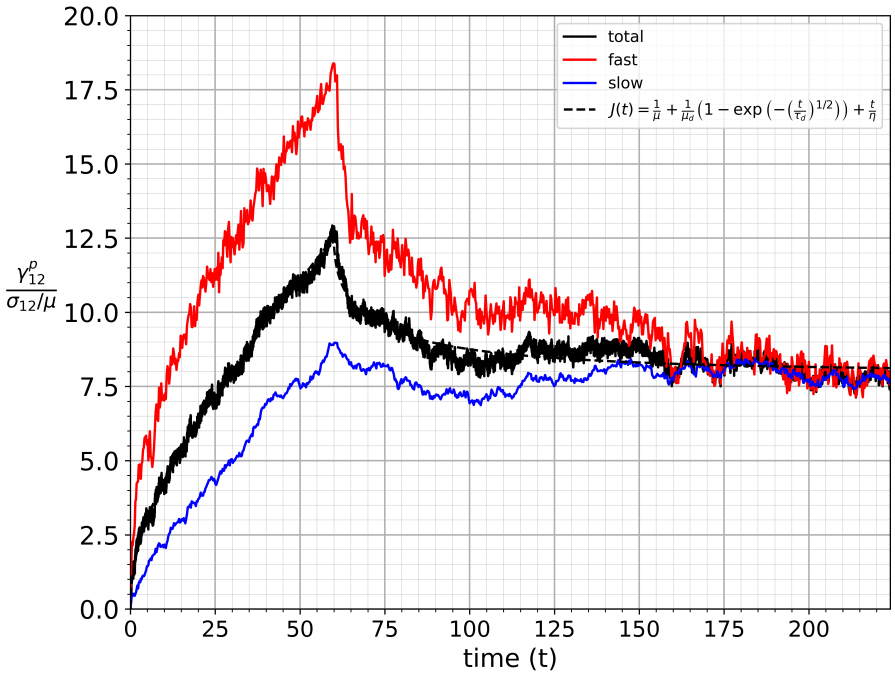


***Figure 13. Viscoelastic fluid model.*** *Normalized inelastic strain ($\gamma^p_{12}(t)/(\sigma_{12}/\mu)$, where $\sigma_{12}$ is the stress applied during creep) vs. time: average values in the fast and slow domains, and global value. The dashed line corresponds to a fit using the creep compliance of Eq.7.*

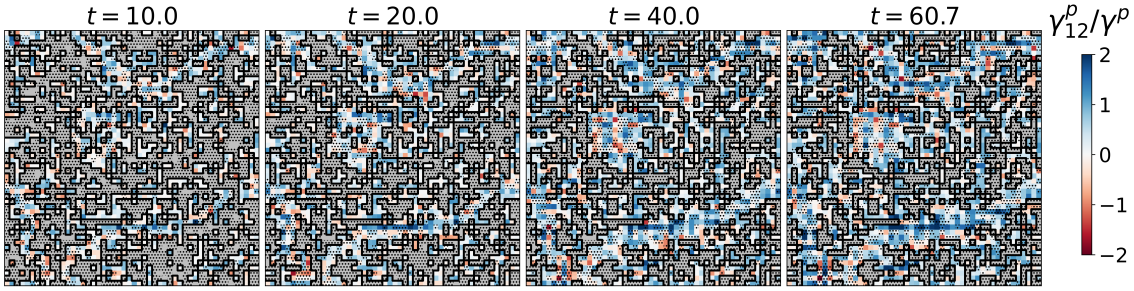


***Figure 14. Viscoelastic fluid model.*** *Inelastic strain map ($\gamma^p_{12}(x_1, x_2, t)$) normalized by the inelastic distortion of a ST ($\gamma^p$) during creep at various step time. The dotted domains correspond to the slow domains. The black lines delineate the boundary between the gray domains where no ST has ever occurred since the beginning of creep and those where STs have occurred. $\gamma^p_{12}(x_1, x_2, t)$ is calculated from the reference state ($t = 0$).*

positive for larger stresses. Consequently, in the framework of linear viscoelasticity ($\gamma^p >> \sigma_{12}/\mu$), once a ST has occurred, it suffers from a relatively large back stress. The square shape used for STZs here, and the under plane-stress conditions, result in a back stress of $\sigma^{STZ}_{12} \sim -40\sigma_{12}$ for a strictly concordant STZ (Fig.19: for $\gamma^p = 0.1$ and $\sigma_{12}/\mu = 0.001$).

As discussed in the introduction, the implications of the existence of this back stress have been widely discussed: if a STZ suffers from a back stress, it would tend to go back to its initial configuration, producing only delayed elasticity but no viscous flow. In order for viscous flow to occur, the back stress must be relieved within the STZ. The most optimal scenario is for neighboring STZs to undergo their own transformations, thereby disturbing and thus relaxing the back stress [50], [85]. Argon was surely the most prolific author in developing a model that finely describes this scenario (see [49] where this model is detailed). Argon postulated that if the long-range stress a STZ induces after its transformation tends to induce transformations of neighboring STZs,

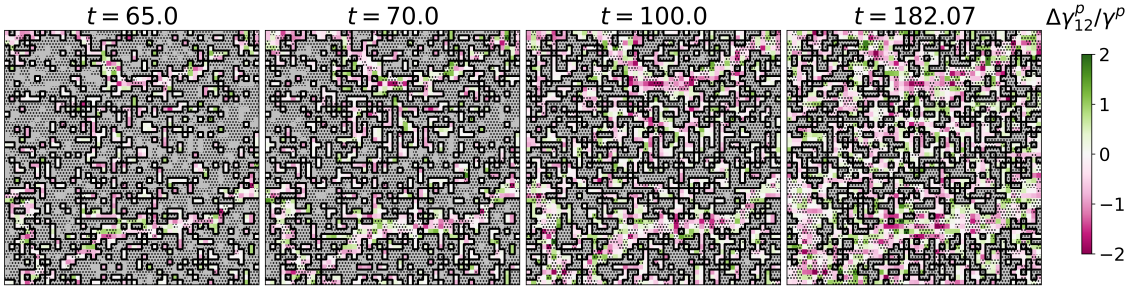


***Figure 15. Viscoelastic fluid model.*** *Inelastic strain map change during recovery ($\Delta\gamma^p_{12}(x_1,x_2,t) = \gamma^p_{12}(x_1,x_2,t) - \gamma^p_{12}(x_1,x_2,t=60.7)$) normalized by the inelastic distortion of a ST ($\gamma^p$) at various step time. Pink domains recovers a part of their inelastic strain, green domains create more inelastic strain. The dotted domains correspond to the slow domains. The black lines delineate the boundary between the gray domains where no ST has ever occurred since the beginning of the recovery ($t = 60.7$) and those where STs have occurred.*

this effect is so minimal that STZ occur randomly and STZ are "spatially isolated" (*i.e.*: a STZ is not necessarily close to the previous one).

Starting from a state where $\sigma_{12}/\mu$ is homogeneous ($= 0.001$, Fig.19), the first STZ, in the Maxwell model, had $1/2500 = 0.04\%$ chance to be selected. Subsequent to its transformation, owing to the back stress, the probability of selection of the same STZ at the next step is estimated to be approximately $14\%$, from Eq.4. Concurrently, its eight neighboring STZ, subject to the Eshelby's stress field, collectively possess an estimated probability of approximately $1\%$ for selection. At greater distances from the initial STZ, the activation rate remains largely unaltered, leading to a probability of approximately $85\%$ for the selection of any other STZ than the first one or its neighborhood. Statistically, the initial STZs are indeed spatially isolated.

Thus Argon stated: "*At this stage, the inelastic deformation is entirely anelastic [...]. Removal of the applied stress renders the back stresses dominant in each site [...] and the sample returns completely to its initial shape*". As the number of randomly located STZ increases, the probability of having one or more ST in close proximity to the initial STZ rises. Argon's calculations indicated that the formation of a cluster of three close STZ results in the relaxation of their back stresses, so that "the memory of the initial unstressed state becomes lost". The deformation of this cluster would now be irreversible. One consequence of this model is that viscous flow arises only after a certain amount of delayed elastic deformation, which occurs after a certain period of time. An implicit assumption of the model is that, at the onset of recovery, only STZs under back stress will recover, while the others remain unaffected. The simulations presented here show a somewhat different story.

## 4.2 Inherent stress heterogeneity

By its inherent disorder a glass is naturally stressed at the microscopic scale [57], at least because its bonds are distorted, but also because once a single thermally activated ST has occurred, it will induce other ST in its neighborhood, maintaining a dynamic and large stress heterogeneity (see [65] for details). Statistically, it is not possible for the system to return to a stress-free state or even a stress state it has previously experienced. The external stress applied during a mechanical test, if it lies in the linear viscoelastic domain, is much more lower than the standard deviation of this inherent stress heterogeneity. As a result, STZs mainly undergo random STs due

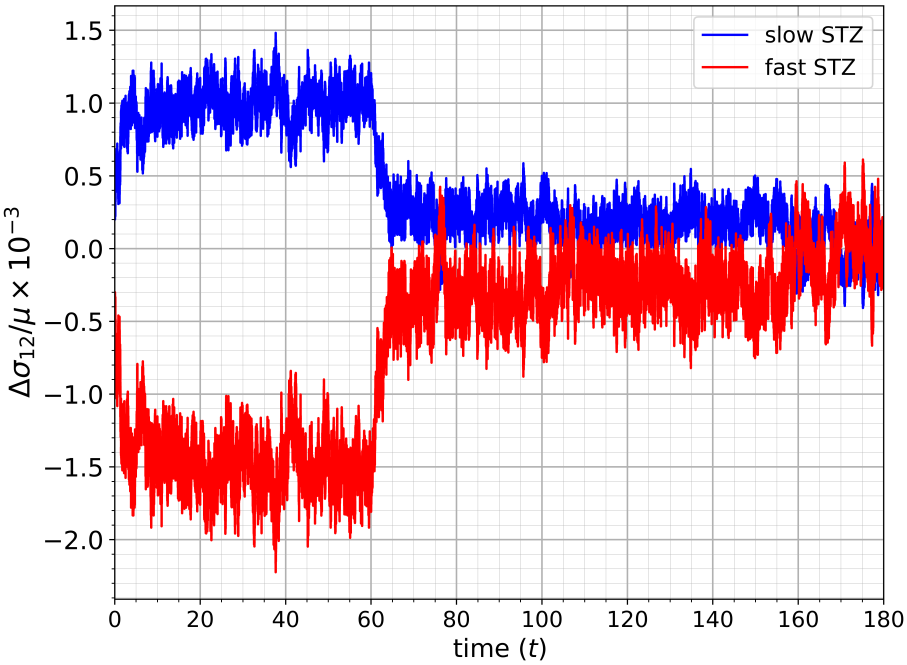


***Figure 16. Viscoelastic fluid model.*** *Difference between the average stresses experienced by the slow ($\sigma_{12}^s$) and fast domains ($\sigma_{12}^f$) and the overall average stress ($\sigma_{12}$): $\Delta\sigma_{12} = \sigma_{12}^s - \sigma_{12}$ and $\Delta\sigma_{12} = \sigma_{12}^f - \sigma_{12}$ respectively, during creep ($\sigma_{12}/\mu = 2.10^{-3}$) and recovery ($\sigma_{12}/\mu = 0$).*

to the dynamic fluctuation of this stress heterogeneity rather than to the macroscopical stress: STs occurring during creep are much more probably totally randomly oriented. The only consequence of the external stress is to induce a very slight bias toward the probability of -partially- concordant STs. It does not mean that STZs are not spatially isolated, but at least that an initial unstressed state does not exist, let alone its memory. On the other hand, once the recovery starts, no STZ is in a state where it doesn't change its inelastic strain anymore. Some STZs can even create extra inelastic strain during recovery, which is balanced by the inelastic strain recovery occurring somewhere else.

### 4.3 How does glass flow?

When a given STZ transforms at an angle $\theta$ (Fig.1), its next transformation will be at an angle $\theta + \Delta\theta$. If $\Delta\theta$ is $\pm 90°$, the STZ recovers exactly its initial configuration. In the Maxwell model, at $\sigma_{12}/\mu = 10^{-3}$, $75\%$ of new transformations occur with $75° < |\Delta\theta| < 105°$ (and roughly an half between $85$ and $95°$). Meaning to say, the majority of the STZ just go back and forth, so still carry on a large part of their back stress until their new transformation: the back stress is dominant in each site and is only very partially relaxed by neighboring transformations. Additionally, if a STZ produces a "very" concordant (arbitrary when $|\theta| < 22.5°$), the probability of his subsequent transformation being also very concordant (*i.e.*: it is only possible if the back stress has almost fully relaxed) is minimal, with a $2.5\%$ chance of occurrence. The scenario depicted by Argon where the memory of the initial unstressed state of a STZ becomes lost before its next transformation is actually an extremely rare situation. In summary, during the creep phase, the increase of inelastic strain is not due to the complete memory loss, that would allow successive concordant STs, but rather to a very partial loss. The increase originates from the fact that if a STZ transformation is often followed by a "backward" one (= almost no memory loss), the latter seldom fully negate the

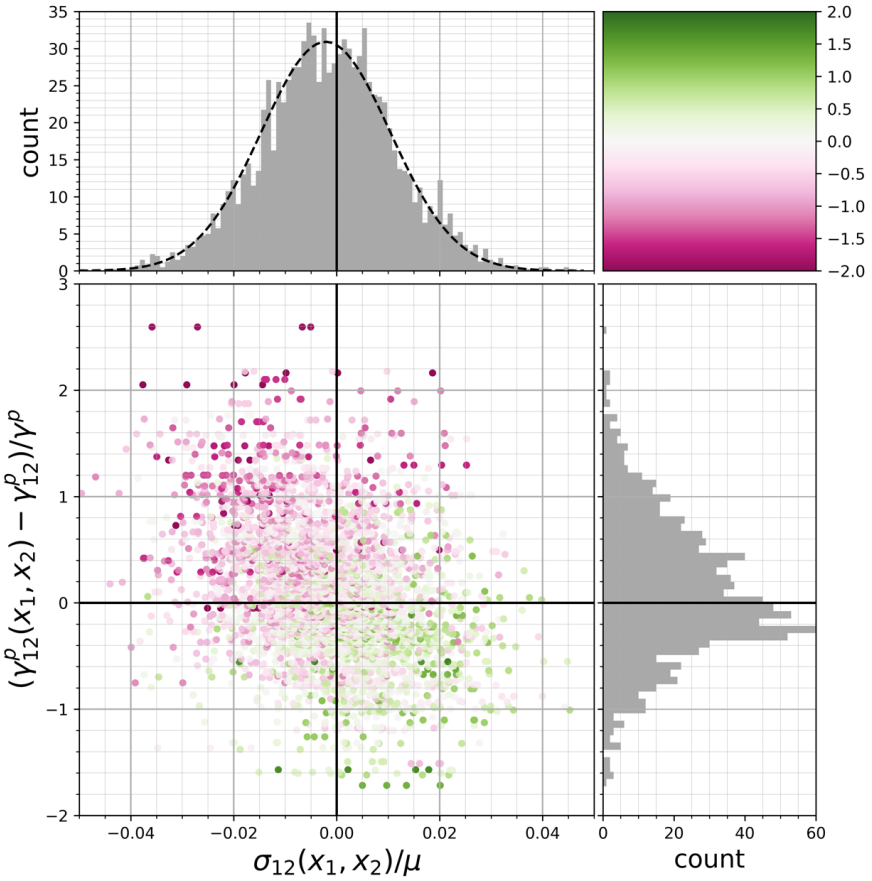


***Figure 17. Viscoelastic fluid model.*** *Inelastic strain excess (relative to the overall average inelastic strain $\gamma^p_{12}/\gamma^p \sim 0.25$) vs. shear stress $\sigma_{12}/\mu$ at the first step of recovery, in every fast STZ. The color scale refers to Fig.15, and corresponds to $\Delta\gamma^p_{12}(t = 182.07)/\gamma^p$ (step: 750 000). The histograms show the number of STZs within each interval, and the black dotted curve represents a Gaussian fit. The stress associated with an STZ is taken as the stress at its central node.*

former, when the former is concordant. While concordant events occur obviously more frequently ($r_{c/d} > 1$) as a result of the stress-induced bias, successive concordant events (complete memory loss) are exceptionally rare.

### 4.4 Delayed elasticity mechanism

Let's first consider the behavior of a rheological model: a Generalized Maxwell Model (GMM) [112] with only two parallel branches, which represents the simplest case where two processes with different relaxation times compete. The creep response, under a constant stress $\sigma$ of this GMM can be described as follows: the "fast" branch, characterized by a short relaxation time ($\tau_f$), creeps more rapidly than the "slow" branch with a longer relaxation time ($\tau_s$). Since both branches experience the same strain, the stress progressively transfers from the fast branch to the slow one until their strain rates become equal, leaving the fast branch with a larger amount of inelastic strain. If both branches possess the same elastic modulus ($\mu$), the characteristic time associated with this stress transfer is $2\ (\tau_f^{-1} + \tau_s^{-1})^{-1}$, and both branches converge, when the fast branch support only a fraction $\tau_f/(\tau_f + \tau_s)$ of $\sigma$, to the same strain rate: $\sigma/(\mu(\tau_f + \tau_s))$. Consequently, if $\tau_s >> \tau_f$, the stress-transfer kinetic is governed by the fast branch, the creep rate is very close to that of the slow branch, and the fast branch tend to support only a very low stress. During recovery, unloading places the fast branch under neg-

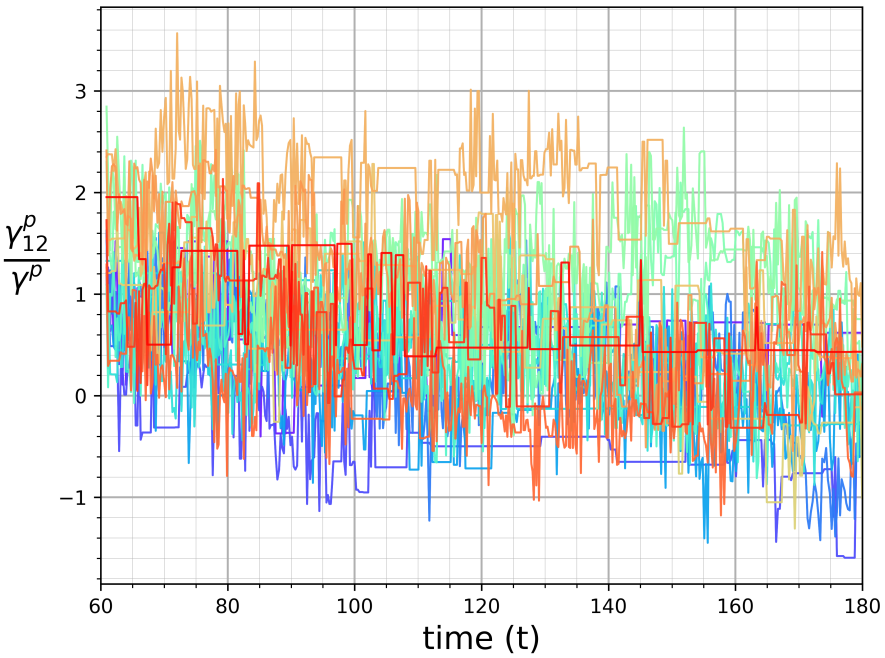


***Figure 18. Viscoelastic fluid model.*** *Inelastic strain evolution during recovery from some selected fast STZs: those having* $\gamma_{12}^p/\gamma^p > 1$ *at the end of creep and recovering more than* $1.5\gamma^p$*.*

ative stress and the slow branch under a smaller positive one. The fast branch thus reduces its inelastic strain ("recovers"), while the slow branch keeps creeping -slowly-, in order to relax their stress. Globally, since the fast branch acts faster, the system recovers, until both branches are stress-free, leaving basically only the inelastic strain the branches have accumulated at equal rates during creep: so effective recovery comes solely from the fast branch. The GMM and the Burger's model share the same creep compliance and relaxation modulus [110]. The viscoelastic fluid model displays macroscopic behavior (creep rates of fast/slow STZs, stress transfer, recovery) qualitatively consistent with that of this rheological model: Its creep compliance corresponds to a Burger model with a broader distribution of retardation times (Eq.7).

A creep and recovery test has two signatures of delayed elasticity: the creep rate doesn't immediately stabilize, and a portion of the strain is recovered once the stress is removed. The creep rate decreases, even though stress and temperature remain constant, because the fastest STZs tend to transfer their stress to the other STZs (Fig.16). The creep rate stabilizes when this stress transfer is complete, since all STZs converge to the same transformation rate. Because fast STZ are initially more active, they tend to undergo more concordant STs, and in return support more back stress, reducing their ability for further concordant STs. On the other hand, the rate of concordant STs of slow STZs should increase, since they support more and more stress. From the GMM equation, it can nevertheless be deduced that because slow STZs are much slower than fast ones, their increase in transformation rate is expected to be barely noticeable.

However, as illustrated in Fig.16 the amplitude of stress transferred from fast to slow STZs is much smaller than the amplitude of the inherent stress heterogeneity: Only a few of the fast STZ are, by the end of stress transfer, under a long-lived back stress, and only few of the slow STZ under a long-lived "forward" stress. All together fast STZs support less and less stress (and vice-versa for slow STZs), but individually, they undergo a randomly fluctuating stress, they do not accumulate back-stress that could stand for their "memory". This memory is collective, not local.

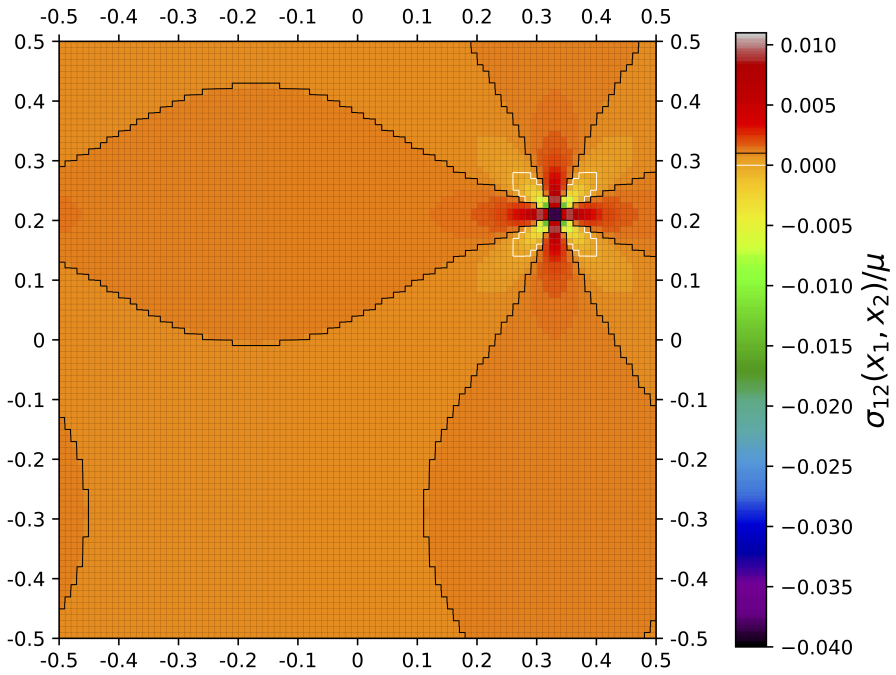


***Figure 19.*** *Shear stress field $\sigma_{12}(x_1, x_2)/\mu$ (element field) after the first ST in the Maxwell model, at the first step of creep ($\sigma_{12}/\mu = 10^{-3}$), without stabilization. The grid is the mesh. The thick black lines is the iso-value line $\sigma_{12}(x_1, x_2)/\mu = 10^{-3}$; the thick white line is the iso-value line $\sigma_{12}(x_1, x_2) = 0$, highlighting the small domain where the stress is now negative.*

At the onset of recovery, fast STZs have transferred most of their stress to slow STZs. As a result, fast STZs collectively carry less stress than the applied creep stress $\sigma_{12}$, while slow STZs carry more. Initiating recovery corresponds to changing the applied stress by $-\sigma_{12}$, leaving the fast STZ under a negative stress. This negative stress acts as the driving force for the partial recovery of their inelastic strain. This is the memory, depicted by Mazurin [86], behind delayed elasticity. Nevertheless, the stress carried by fast STZ is broadly distributed: first, not all fast STZs experience a negative stress, and second, there is no strong correlation between the stress supported by a given STZ at the onset of recovery and the amount of inelastic strain it eventually recovers. Once again, the memory is not stored locally at the level of an individual STZ, but is instead collective. The memory being not local, it is transferred over time from one STZ to another through the long-range stress field induced by individual shear transformations. The memory is ultimately lost when the fast STZs have relaxed the negative stress they were collectively carrying at the onset of recovery.

Only a few STZs carry memory on their own: those with a large excess of inelastic strain (much larger than $\gamma^p$). They bear a large back stress at the onset of recovery and relax it by recovering their inelastic strain. Most STZs instead undergo back-and-forth transformations that, taken together, give rise to the global recovery. This particular situation is highlighted in the Maxwell model, where STZs with a large excess of inelastic strain localize into bands; in this case, fast STZs are self-created. When fast STZs exist intrinsically, such localization does not occur, because they are homogeneously distributed, and only a tiny fraction of STZs recover continuously once the creep stress is removed.

### 4.5 Effects of STZ shape and activation direction

It should be noted that STs do not necessarily occur in the direction of the maximal shear stress supported by the corresponding STZ. They can occur in "random directions" because they are mainly thermally activated [65], [88], [89]. A STZ only occurs statistically in a direction concordant with the stress it supports. As explained in the previous paragraphs, a given ST is fairly inefficient to contribute to the macroscopical flow, because STZs mainly transform back and forth with a very small accumulation a inelastic distortion per "round trip". It is more realistic to consider that the direction of each transformation is also statistical, as proposed by Homer *et al.* [65], [88], but it means considering/simulating more neutral transformations ($\theta \rightarrow \pm\pi/4$, Figure 1), which have obviously no effect on macroscopical flow: this makes the simulation even slower to produce a significant macroscopic deformation $\gamma_{12}^p$. Additionally, owing to the square geometry of the STZ considered here, the probability of STs occurring along a direction defined by an angle $\theta$ ($p(\theta)$) is not isotropic in the absence of macroscopic stress. It can be expressed as:

$$\frac{p(\theta) - p(0)}{p(0)} = (\sqrt{2} - 1)\, e^{-\frac{(|\theta| - \pi/4)^2}{2s^2}} \tag{8}$$

This relation indicates that shear transformations oriented along $|\theta| = \pi/4$ are $\sqrt{2}$ times more likely than those occurring at $\theta = 0$, following a Gaussian distribution centered around this preferential direction (standard deviation: $s = \pi/12$). When a macroscopic shear stress is applied, this distribution becomes slightly linearly tilted: concordant events ($\theta = 0$) become more probable, whereas discordant events ($|\theta| = \pi/2$) become less probable. In other words, the square geometry of the STZ promotes neutral events. In this context, explicitly accounting for additional randomly oriented transformations appears unnecessary, as the variability of the activation process, together with the geometrical bias of the STZ, already leads to sufficiently disordered dynamics. This contribution has therefore been deliberately omitted from the present analysis.

The viscosity in the linear viscoelastic (Newtonian) regime can be estimated from the well-known expression reported by Homer *et al.* [65] (their Eq.17), which is rewritten here using the dimensionless variables introduced in the present work:

$$\frac{\eta}{\mu} = \frac{\sigma_{12}/\mu}{2\gamma^p \sinh\left(a\frac{\sigma_{12}}{\mu}\right)} \sim \frac{1}{2a\gamma^p} \tag{9}$$

For $a = 150$, this approximation yields $\eta/\mu \sim 0.03$ (in dimensionless time units). By comparison, the Maxwell model developed here gives $\eta/\mu = 1/3.6 \sim 0.28$, *i.e.* a value less than one order of magnitude larger. The model of Homer *et al.* [65], which relies on similar activation mechanisms for STZs, predicts a viscosity about 3 times larger than estimated from the above equation at equivalent $a$.Therefore, the present model remains in quite good agreement with the one of Homer *et al.*, despite the simplified geometry adopted here (square-shaped STZs).

### 4.6 Delayed elasticity vanishing

In the glass transition domain, glasses relax their stress at constant strain following a stretched exponential decay [81]. At higher temperatures, the stretched exponent increases, tending to an exponential relaxation. This phenomenon indicates the van-

ishing of delayed elasticity [78]. As the temperature increases, the activation rate of STs rises concomitantly with a decrease in the elastic moduli [113], and thus the celerity of mechanical waves. It leads to an increase in the time required for the stress field to propagate over a large distance after a ST, while concurrently decreasing the delay before new transformation in the vicinity. A ST can occur prior to being influenced by previous STs. On this basis, I suggest that the delayed elasticity, which is the result of the interaction between STZs via a long-range stress field, disappears because of this loss of interactions.

## 5. Conclusion

Delayed elasticity is a universal feature of amorphous solids in their glass transition domain. This universality implies that the observed viscoelastic behavior does not arise from atomic-scale details or from the material's chemical composition. Accordingly, a mesoscopic modeling approach is particularly appropriate for uncovering the mechanisms underlying delayed elasticity. Such models, based on local shear transformations (ST), were initiated by Bulatov and Argon [87], further developed by Homer *et al.* [65], [88], and more recently by Van Loock *et al.* [89], with the aim of modeling the inelastic behavior of metallic glasses. I have adopted here this modeling framework, and removed all features specific to metallic glasses or thermal history, in order to investigate the universal origin of delayed elasticity in a regime that has been largely unexplored by these models: the linear viscoelastic domain.

Any "realistic" glass cannot be considered pristine with respect to prior STs, since such events are thermally activated and inevitably occur before any mechanical testing. In the simulations, the system is first equilibrated to suppress aging effects during mechanical testing, by allowing it to undergo a sufficient number of spontaneous STs until their activation rate stabilizes. In this state, the system reaches a dynamic equilibrium characterized by large, spatially heterogeneous stress fluctuations of stable amplitude. The simulations show that the linear viscoelastic domain lies within a macroscopic stress range smaller than this amplitude. In this domain, the stress favors transformations aligned with its direction (concordant) and disfavors those opposed (discordant), without increasing the overall transformation frequency.

The classical heuristic interpretation of the origin of delayed elasticity is the following [4], [40], [48], [50], [78], [85], [91]: when a ST occurs, if the corresponding shear strain is much larger than the macroscopic strain applied, the transformed zone undergoes a back stress, which tends to drive it back toward its initial configuration. If the back stress is disrupted by subsequent ST in the surrounding domain, the memory of the initial configuration is lost, leading to viscous deformation. Conversely, if the back stress is preserved, the transformed region can recover its original state upon removal of the macroscopic stress and this recovery is the manifestation of delayed elasticity.

Because the material remains in dynamic stress equilibrium, the mechanical memory cannot be stored locally. Instead, back stresses are continuously transferred between STZs through the long-range stress fields generated by individual STs. In the presence of a distribution of activation energies, fast STZs (with low energy barriers) collectively transfer the fraction of macroscopic stress they initially support to slower STZs, and therefore sustain back stress in a collective rather than individual manner. As a result, the "memory" associated with delayed elasticity is distributed among fast STZs and fluctuates both spatially and temporally. Delayed elasticity should therefore not be interpreted in terms of individual STZs accumulating back stress during creep

and releasing it continuously during recovery. Rather, it emerges as a collective phenomenon, which can exist only if long-range interactions between STZs are effective, *i.e.*, if the glass retains significant shear elasticity.

## Data availability statement

Due to the large volume of data associated with each simulation, the data supporting the findings of this study are available from the author upon reasonable request. The code is provided as Supplementary Material and is available at:
https://doi.org/10.5281/zenodo.19369590

## Author contributions

Y.Gueguen: Conceptualization, Data curation, Formal Analysis, Investigation, Methodology, Validation, Visualization, Writing.

## Competing interests

The author declares that he has no competing interests.

## Acknowledgements

I am indebted to Prof. Vincent Keryvin (Univ. Bretagne Sud, UMR CNRS 6027, IRDL) for proofreading the manuscript and improving its clarity.

## References

[1] U. Fotheringham, "Viscosity of glass and glass-forming melts," in *Springer handbook of glass*, Springer, 2019, pp. 79–112.

[2] L. Boltzmann, "On the theory of the elastic aftereffect," *Poggendorff's Ann. Phys. Chem*, vol. 7, pp. 624–645, 1876.

[3] R. Simha, "On Relaxation Effects in Amorphous Media," *J. Appl. Phys.*, vol. 13, no. 3, pp. 201–207, 1942. DOI: 10.1063/1.1714856.

[4] A. S. Argon, "Mechanisms of inelastic deformation in metallic glasses," *J. Phys. Chem. Solids*, vol. 43, no. 10, pp. 945–961, 1982. DOI: 10.1016/0022-3697(82)90111-1.

[5] A. O. Rankine, "The behaviour of over-strained materials," *Science Progress in the Twentieth Century (1906-1916)*, vol. 1, no. 3, pp. 465–482, 1907. [Online]. Available: https://www.jstor.org/stable/43769106.

[6] W. Weber, "Ueber die elasticität der seidenfäden," *Ann. Phys. (Berl.)*, vol. 110, no. 2, pp. 247–257, Jan. 1835, ISSN: 1521-3889. DOI: 10.1002/andp.18351100204.

[7] W. Weber, "Ueber die elasticitäet fester körper," *Ann. Phys. (Berl.)*, vol. 130, no. 9, pp. 1–18, 1841. DOI: 10.1002/andp.18411300902.

[8] H. Cavendish, "XXI. experiments to determine the density of the earth," *Philos. Trans. R. Soc. Lond.*, vol. 88, pp. 469–526, 1798, see p.478. DOI: 10.1098/rstl.1798.0022.

[9] C. W. F. Everitt, "Gravitation, relativity and precise experimentation," in *Proc. of the First Marcel Grossmann Meeting on General Relativity*, 1977, pp. 545–615. [Online]. Available: https://einstein.stanford.edu/content/sci_papers/papers/Everitt_Gravitation-Precise-Expt-1977.pdf.

[10] F. Kohlrausch, "Ueber die elastische nachwirkung bei der torsion," *Annalen der physik*, vol. 195, no. 7, pp. 337–368, 1863. DOI: 10.1002/andp.18631950702.

[11] L. Boltzmann, *Zur Theorie der elastischen Nachwirkung , Sitzungsberichte der Mathematisch-Naturwissenschaftlichen Classe der Kaiserlichen Akademie der Wissenschaften, 70 (2): 275–306*, 1874. DOI: 10.1017/CBO9781139381420.031.

[12] O. E. Meyer, "Theorie der elastischen Nachwirkung," *Annalen der Physik*, vol. 227, no. 1, pp. 108–119, 1874. DOI: 10.1002/ANDP.18742270106.

[13] E. Wiechert, "Gesetze der elastischen nachwirkung für constante temperatur," *Ann. Phys. (Berl.)*, vol. 286, no. 11, pp. 546–570, 1893. DOI: 10.1002/andp.18932861110.

[14] M. Dörries, "Prior History and Aftereffects: Hysteresis and "Nachwirkung" in 19th-Century Physics," *Historical studies in the physical and biological sciences*, vol. 22, no. 1, pp. 25–55, 1991. DOI: 10.2307/27757672.

[15] M. G. Ianniello, "Elastic Nachwirkung, Brownian motion, and the tide against determinism: 1835-1920," *Historical studies in the physical and biological sciences*, vol. 24, no. 1, pp. 41–100, 1993. DOI: 10.2307/27757712.

[16] B. B. DeWitt, "On the transparency of the ether," *Nebraska University Studies*, vol. I, no. I, pp. 1–17, 1888. [Online]. Available: https://digitalcommons.unl.edu/cgi/viewcontent.cgi?article=1002&context=univstudiespapers.

[17] H. Lamb, "On a certain theory of elastic after-strain," *Nature*, vol. 41, no. 1064, pp. 463–463, 1890. DOI: 10.1038/041463b0.

[18] H. Markovitz, "Boltzmann and the Beginnings of Linear Viscoelasticity," *T. Soc. Rheol.*, vol. 21, no. 3, pp. 381–398, Sep. 1977. DOI: 10.1122/1.549444.

[19] K. E. Guthe, "Some peculiarities in the elastic properties of certain substances," in *Proceedings of the Iowa Academy of Science*, vol. 15, 1908, pp. 147–156. [Online]. Available: https://scholarworks.uni.edu/pias/vol15/iss1/24.

[20] E. C. Bingham, "Plasticity and elasticity," *J. Franklin Inst. B*, vol. 197, no. 1, pp. 99–115, 1924, ISSN: 0016-0032. DOI: https://doi.org/10.1016/S0016-0032(24)90500-X.

[21] K. H. Borchard, "Elastic after-effect in glass," *Sprechsaal*, vol. 67, no. 20, p. 297, 1934.

[22] W. Thomson, *Elasticity and heat*. Adam and Charles Black, 1878.

[23] W. T. B. Kelvin, *Mathematical and Physical Papers*. At the University Press, 1890, vol. 3.

[24] A. Love, *A treatise on the mathematical theory of elasicity*. Cambrigde: at the university press, 1892, vol. Vol.1, p. 103. [Online]. Available: https://hal.science/hal-01307751v1/file/LoveVol1.pdf.

[25] E. Bergler, "Contributions to the theory of glass formation and the glassy state," *J. Am. Ceram. Soc.*, vol. 15, no. 12, pp. 647–678, 1932. DOI: 10.1111/j.1151-2916.1932.tb13902.x.

[26] M. F. Sayre, "Elastic after-effect in metals," *J. Rheol.*, vol. 3, no. 2, pp. 206–211, Apr. 1932, ISSN: 0097-0360. DOI: 10.1122/1.2116452.

[27] F. W. Preston, "The time factor in the testing of glassware," *J. Am. Ceram. Soc.*, vol. 18, no. 1-12, pp. 220–224, 1935. DOI: 10.1111/j.1151-2916.1935.tb19384.x.

[28] N. W. Taylor, "Mechanism of fracture of glass and similar brittle solids," *J. Appl. Phys.*, vol. 18, no. 11, pp. 943–955, 1947. DOI: 10.1063/1.1697579.

[29] D. Griggs, "Creep of rocks," *The Journal of Geology*, vol. 47, no. 3, pp. 225–251, 1939. DOI: 10.1086/624775.

[30] A. A. Michelson, "The laws of elastico-viscous flow," *Proc. Natl. Acad. Sci.*, vol. 3, no. 5, pp. 319–323, May 1917, ISSN: 1091-6490. DOI: 10.1073/pnas.3.5.319.

[31] C. W. Washburne, "Some wrong words," *The Journal of Geology*, vol. 51, no. 7, pp. 495–497, 1943. DOI: 10.1086/625173.

[32] G. Wiedemann, "I. On torsion," *The London, Edinburgh, and Dublin Philosophical Magazine and Journal of Science*, vol. 9, no. 53, pp. 1–15, 1880. DOI: 10.1080/14786448008626791.

[33] C. Barus, *Maxwell's theory of the viscosity of solids and certain features of its physical verification*. 1888. DOI: 10.2475/ajs.s3-36.213.178.

[34] W. J. M. Rankine, *A Manual of applied Mechanics: With numerous Diagrams*. Ch. Griffin, 1876.
[35] M. H. Tresca, "On further applications of the flow of solids," *Proceedings of the Institution of Mechanical Engineers*, vol. 29, no. 1, pp. 301–345, 1878. DOI: 10.1016/0016-0032(78)90311-3.
[36] G. J. Bair, "II, the correlation of physical properties with atomic arrangement," *J. Am. Ceram. Soc.*, vol. 19, no. 1–12, pp. 347–358, Jan. 1936, ISSN: 1551-2916. DOI: 10.1111/j.1151-2916.1936.tb19849.x.
[37] N. W. Taylor and P. S. Dear, "Elastic and viscous properties of several soda-silica glasses in the annealing range of temperature," *J. Am. Ceram. Soc.*, vol. 20, no. 1-12, pp. 296–304, 1937. DOI: 10.1111/j.1151-2916.1937.tb19906.x.
[38] N. W. Taylor, "Anomalous flow in glasses," *J. Phys. Chem.*, vol. 47, no. 3, pp. 235–253, Mar. 1943, ISSN: 1541-5740. DOI: 10.1021/j150426a004.
[39] G. O. Jones, "Viscosity and related properties in glass," *Rep. Prog. Phys.*, vol. 12, no. 1, p. 133, Jan. 1949. DOI: 10.1088/0034-4885/12/1/307.
[40] A. S. Argon, "Delayed elasticity in inorganic glasses," *J. Appl. Phys.*, vol. 39, no. 9, pp. 4080–4086, 1968. DOI: 10.1063/1.1656927.
[41] C. M. Zener and S. Siegel, "Elasticity and anelasticity of metals," *J. Phys. Chem.*, vol. 53, no. 9, pp. 1468–1468, 1949. DOI: 10.1021/j150474a017.
[42] C. Zener and J. H. Hollomon, "Problems in non-elastic deformation of metals," *J. Appl. Phys.*, vol. 17, no. 2, pp. 69–82, Feb. 1946, ISSN: 1089-7550. DOI: 10.1063/1.1707696.
[43] J. V. Fitzgerald, "Anelasticity of glass: I, introduction," *J. Am. Ceram. Soc.*, vol. 34, no. 10, pp. 314–319, 1951. DOI: 10.1111/j.1151-2916.1951.tb13475.x.
[44] J. V. Fitzgerald, "Anelasticity of glass: II, internal friction and sodium ion diffusion in tank plate glass, a typical soda-lime-silica glass," *J. Am. Ceram. Soc.*, vol. 34, no. 11, pp. 339–342, 1951. DOI: 10.1111/j.1151-2916.1951.tb13481.x.
[45] J. V. Fitzgerald, "Anelasticity of glass: III, effect of heat-treatment on the internal friction of tank plate glass," *J. Am. Ceram. Soc.*, vol. 34, no. 12, pp. 388–390, 1951. DOI: 10.1111/j.1151-2916.1951.tb13020.x.
[46] J. V. Fitzgerald, "Anelasticity of glass: IV, correlation of electrical strain with mechanical strain in glass," *J. Am. Ceram. Soc.*, vol. 34, no. 12, pp. 390–391, 1951. DOI: 10.1111/j.1151-2916.1951.tb13021.x.
[47] L. C. Hoffman, "Chemical composition and the anelasticity of glass," Ph.D. dissertation, The Pennsylvania State University, 1952.
[48] A. S. Argon, "Investigations of the Strength and Anelasticity of Glass," Ph.D. dissertation, Massachusetts Institute of Technology, 1956. [Online]. Available: https://dspace.mit.edu/handle/1721.1/57750.
[49] A. S. Argon and L. T. Shi, "Development of visco-plastic deformation in metallic glasses," *Acta Metall.*, vol. 31, no. 4, pp. 499–507, 1983. DOI: 10.1016/0001-6160(83)90038-X.
[50] M. Goldstein, "Viscous liquids and the glass transition: A potential energy barrier picture," *J. Chem. Phys.*, vol. 51, pp. 3728–3739, 1969. DOI: 10.1063/1.1672587.
[51] S. Parke, "Anelasticity and viscoelasticity in glass," *British Journal of Applied Physics*, vol. 14, no. 5, pp. 243–248, 1963. DOI: 10.1088/0508-3443/14/5/306.
[52] E. C. Bingham, *Fluidity and plasticity*. McGraw-Hill, 1922.
[53] R. Hill, *The mathematical theory of plasticity*. Oxford university press, 1998, vol. 11.
[54] A. Nicolas, E. E. Ferrero, K. Martens, and J.-L. Barrat, "Deformation and flow of amorphous solids: Insights from elastoplastic models," *Rev. Mod. Phys.*, vol. 90, no. 4, p. 045 006, 2018. DOI: 10.1103/RevModPhys.90.045006.
[55] D. Rodney, A. Tanguy, and D. Vandembroucq, "Modeling the mechanics of amorphous solids at different length scale and time scale," *Model. Simul. Mater. Sci. Eng.*, vol. 19, no. 8, p. 083 001, 2011. DOI: 10.1088/0965-0393/19/8/083001.

[56] K. E. Jensen, D. A. Weitz, and F. Spaepen, "Local shear transformations in deformed and quiescent hard-sphere colloidal glasses," *Phys. Rev. E*, vol. 90, no. 4, p. 042 305, 2014. DOI: 10.1103/PhysRevE.90.042305.

[57] A. Tanguy, "Elasto-plastic behavior of amorphous materials: A brief review," *C. R. Phys.*, vol. 22, no. S3, pp. 1–17, 2021. DOI: 10.5802/crphys.49.

[58] T. Rouxel, H. Ji, V. Keryvin, T. Hammouda, and S. Yoshida, "Poisson's ratio and the glass network topology-relevance to high pressure densification and indentation behavior," *Adv. Mater. Res.*, vol. 39, pp. 137–146, 2008. DOI: 10.4028/www.scientific.net/AMR.39-40.137.

[59] T. Rouxel, H. Ji, T. Hammouda, and A. Moréac, "Poisson's ratio and the densification of glass under high pressure," *Physical Review Letters*, vol. 100, no. 22, p. 225 501, 2008. DOI: 10.1103/PhysRevLett.100.225501.

[60] K. W. Peter, "Densification and flow phenomena of glass in indentation experiments," *J. Non-Cryst. Solids*, vol. 5, no. 2, pp. 103–115, 1970. DOI: 10.1016/0022-3093(70)90188-2.

[61] E. Barthel, V. Keryvin, G. Rosales-Sosa, and G. Kermouche, "Indentation cracking in silicate glasses is directed by shear flow, not by densification," *Acta Mater.*, vol. 194, pp. 473–481, 2020, ISSN: 1359-6454. DOI: https://doi.org/10.1016/j.actamat.2020.05.011.

[62] B. Mantisi, A. Tanguy, G. Kermouche, and E. Barthel, "Atomistic response of a model silica glass under shear and pressure," *Eur. Phys. J. B*, vol. 85, no. 9, p. 304, 2012. DOI: 10.1140/epjb/e2012-30317-6.

[63] J. T. Hagan, "Shear deformation under pyramidal indentations in soda-lime glass," *J. Mater. Sci.*, vol. 15, no. 6, pp. 1417–1424, 1980. DOI: 10.1007/BF00752121.

[64] T. Rouxel and J.-C. Sanglebœuf, "The brittle to ductile transition in a soda - lime - silica glass," *J. Non-Cryst.*, vol. 271, no. 3, pp. 224–235, 2000. DOI: 10.1016/S0022-3093(00)00109-5.

[65] E. R. Homer and C. A. Schuh, "Mesoscale modeling of amorphous metals by shear transformation zone dynamics," *Acta Mater.*, vol. 57, no. 9, pp. 2823–2833, 2009. DOI: 10.1016/j.actamat.2009.02.035.

[66] W. A. Zdaniewski, G. E. Rindone, and D. E. Day, "The internal friction of glasses," *J. Mater. Sci.*, vol. 14, no. 4, pp. 763–775, 1979. DOI: 10.1007/bf00550707.

[67] S. Reinsch, R. Müller, J. Deubener, and H. Behrens, "Internal friction of hydrated soda-lime-silicate glasses," *J. Chem. Phys.*, vol. 139, no. 17, p. 174 506, Nov. 2013. DOI: 10.1063/1.4828740.

[68] S. V. Borovinskii and O. V. Mazurin, "On the concept of volume viscosity," in *Progress and Trends in Rheology II: Proceedings of the Second Conference of European Rheologists, Prague, June 17–20, 1986*, Springer, 1988, pp. 79–81. DOI: 10.1007/978-3-642-49337-9_16.

[69] J. J. Mills and J. L. Sievert, "Stress relaxation modulus of a commercial glass," *J. Am. Ceram. Soc.*, vol. 56, no. 10, pp. 501–505, 1973. DOI: 10.1111/j.1151-2916.1973.tb12397.x.

[70] M. J. Crochet, J. De Bast, P. Gilard, and G. Tackels, "Experimental study of stress relaxation during annealing," *J. Non-Cryst. Solids*, vol. 14, no. 1, pp. 242–254, 1974. DOI: 10.1016/0022-3093(74)90033-7.

[71] M. S. Rekhson and S. M. Rekhson, "Shear, uniaxial, and biaxial stress relaxation functions," *J. Am. Ceram. Soc.*, vol. 69, no. 9, pp. 704–708, 1986. DOI: 10.1111/j.1151-2916.1986.tb07475.x.

[72] S. M. Rekhson, "Chapter 1 - Viscoelasticity of Glass," in *Viscosity and Relaxation*, ser. Glass Science and Technology, D. Uhlmann and N. Kreidl, Eds., vol. 3, Elsevier, 1986, pp. 1–117. DOI: 10.1016/B978-0-12-706703-2.50004-0.

[73] L. Duffrène, R. Gy, H. Burlet, and R. Piques, "Multiaxial linear viscoelastic behavior of a soda - lime - silica glass based on a generalized maxwell model," *J. Rheol.*, vol. 41, no. 5, pp. 1021–1038, Sep. 1997. DOI: 10.1122/1.550824.

[74] F. T. Trouton, "On the coefficient of viscous traction and its relation to that of viscosity," *Proc. R. Soc. London A.*, vol. 77, no. 519, pp. 426–440, 1906. DOI: 10.1098/rspa.1906.0038.

[75] L. Li, E. R. Homer, and C. A. Schuh, "Shear transformation zone dynamics model for metallic glasses incorporating free volume as a state variable," *Acta Mater.*, vol. 61, no. 9, pp. 3347–3359, 2013. DOI: 10.1016/j.actamat.2013.02.024.

[76] P. Debye, "Einige resultate einer kinetischen theorie der isolatoren," *Physik Z.*, vol. 13, p. 97, 1912.

[77] J. C. Maxwell, "On the dynamical theory of gases," *Philos. Trans. R. Soc. London*, vol. 157, pp. 49–88, 1867. [Online]. Available: http://www.jstor.org/stable/108968.

[78] Y. Gueguen et al., "A relationship between non-exponential stress relaxation and delayed elasticity in the viscoelastic process in amorphous solids: Illustration on a chalcogenide glass," *Mech. Mater.*, vol. 85, pp. 47–56, 2015. DOI: 10.1016/j.mechmat.2015.02.013.

[79] R. Becker, "Elastische nachwirkung und plastizität," *Zeitschrift für Physik*, vol. 33, no. 1, pp. 185–213, 1925.

[80] R. C. Welch et al., "Dynamics of glass relaxation at room temperature," *Phys. Rev. Lett.*, vol. 110, p. 265 901, 26 Jun. 2013. DOI: 10.1103/PhysRevLett.110.265901.

[81] R. Böhmer, K. L. Ngai, C. A. Angell, and D. J. Plazek, "Nonexponential relaxations in strong and fragile glass formers," *J. Chem. Phys.*, vol. 99, no. 5, pp. 4201–4209, Sep. 1993. DOI: 10.1063/1.466117.

[82] T. Mura, "General theory of eigenstrains," *Micromechanics of defects in solids*, pp. 1–73, 1987. DOI: 10.1007/978-94-009-3489-4_1.

[83] J. D. Eshelby, "The determination of the elastic field of an ellipsoidal inclusion, and related problems," *Proceedings of the royal society of London. Series A. Mathematical and physical sciences*, vol. 241, no. 1226, pp. 376–396, 1957. DOI: 10.1098/rspa.1957.0133.

[84] J. Chattoraj and A. Lemaitre, "Elastic signature of flow events in supercooled liquids under shear," *Phys. Rev. Lett.*, vol. 111, no. 6, p. 066 001, 2013. DOI: 10.1103/PhysRevLett.111.066001.

[85] E. Orowan, "Creep in metallic and non-metallic materials.," *Proc. First U.S. Natn. Cong. Appl. Mech.*, 453–47, New York: ASME, 1952.

[86] O. V. Mazurin, "Glass relaxation," *J. Non-Cryst. Solids*, vol. 87, no. 3, pp. 392–407, 1986. DOI: 10.1016/S0022-3093(86)80013-8.

[87] V. V. Bulatov and A. S. Argon, "A stochastic model for continuum elasto-plastic behavior. I. Numerical approach and strain localization," *Modelling and Simulation in Materials Science and Engineering*, vol. 2, no. 2, p. 167, 1994. DOI: 10.1088/0965-0393/2/2/001.

[88] E. R. Homer, D. Rodney, and C. A. Schuh, "Kinetic Monte Carlo study of activated states and correlated shear-transformation-zone activity during the deformation of an amorphous metal," *Phys. Rev. B*, vol. 81, p. 064 204, 6 Feb. 2010. DOI: 10.1103/PhysRevB.81.064204.

[89] F. Van Loock, L. Brassart, and T. Pardoen, "Implementation and calibration of a mesoscale model for amorphous plasticity based on shear transformation dynamics," *Int. J. Plasticity*, vol. 145, p. 103 079, 2021. DOI: 10.1016/j.ijplas.2021.103079.

[90] V. Keryvin, "Indentation as a probe for pressure sensitivity of metallic glasses," *J. Phys. Condens. Matter*, vol. 20, no. 11, p. 114 119, Feb. 2008. DOI: 10.1088/0953-8984/20/11/114119.

[91] A. S. Argon, "Plastic deformation in metallic glasses," *Acta Metall.*, vol. 27, no. 1, pp. 47–58, 1979. DOI: 10.1016/0001-6160(79)90055-5.

[92] D. F. Castellanos and M. Zaiser, “Avalanche behavior in creep failure of disordered materials,” *Phys. Rev. Lett.*, vol. 121, p. 125 501, 12 2018. DOI: 10.1103/PhysRevLett.121.125501.
[93] D. F. Castellanos and M. Zaiser, “Statistical dynamics of early creep stages in disordered materials,” *Eur. Phys. J. B*, vol. 92, pp. 1–12, 2019. DOI: 10.1140/epjb/e2019-100124-0.
[94] Q. Hao et al., “Decoupling elasticity, anelasticity, and plasticity in static and dynamic stress relaxation of metallic glasses,” *Sci. China Technol. Sci.*, vol. 68, no. 9, p. 1 920 203, 2025. DOI: 10.1007/s11431-025-2970-4.
[95] A. S. Argon and H. Y. Kuo, “Free energy spectra for inelastic deformation of five metallic glass alloys,” *J. Non-Cryst. Solids*, vol. 37, no. 2, pp. 241–266, 1980. DOI: 10.1016/0022-3093(80)90155-6.
[96] P. Schall, D. A. Weitz, and F. Spaepen, “Structural rearrangements that govern flow in colloidal glasses,” *Science*, vol. 318, no. 5858, pp. 1895–1899, 2007. DOI: 10.1126/science.1149308.
[97] J. S. Langer, “Shear-transformation-zone theory of plastic deformation near the glass transition,” *Phys. Rev. E*, vol. 77, no. 2, p. 021 502, 2008. DOI: 10.1103/physreve.77.021502.
[98] J. H. Simmons, R. Ochoa, K. D. Simmons, and J. J. Mills, “Non-newtonian viscous flow in soda-lime-silica glass at forming and annealing temperatures,” *J. Non-Cryst.*, vol. 105, no. 3, pp. 313–322, 1988. DOI: 10.1016/0022-3093(88)90325-0.
[99] C. A. Schuh, T. C. Hufnagel, and U. Ramamurty, “Mechanical behavior of amorphous alloys,” *Acta Mater.*, vol. 55, no. 12, pp. 4067–4109, 2007. DOI: 10.1016/j.actamat.2007.01.052.
[100] F. Puosi, J. Rottler, and J.-L. Barrat, “Time-dependent elastic response to a local shear transformation in amorphous solids,” *Phys. Rev. E*, vol. 89, p. 042 302, 4 Apr. 2014. DOI: 10.1103/PhysRevE.89.042302.
[101] A. Nicolas, F. Puosi, H. Mizuno, and J.-L. Barrat, “Elastic consequences of a single plastic event: Towards a realistic account of structural disorder and shear wave propagation in models of flowing amorphous solids,” *J. Mech. Phys. Solids*, vol. 78, pp. 333–351, 2015. DOI: 10.1016/j.jmps.2015.02.017.
[102] CEA, *Cast3m*, 2022. [Online]. Available: http://www-cast3m.cea.fr.
[103] D. M. Barnett and W. Cai, “Properties of the Eshelby tensor and existence of the equivalent ellipsoidal inclusion solution,” *J. Mech. Phys. Solids*, vol. 121, pp. 71–80, 2018. DOI: 10.1016/j.jmps.2018.07.019.
[104] J. Frenkel, “Über die wärmebewegung in festen und flüssigen körpern,” *Zeitschrift für Physik*, vol. 35, no. 8-9, pp. 652–669, 1926.
[105] S. Sandfeld, Z. Budrikis, S. Zapperi, and D. F. Castellanos, “Avalanches, loading and finite size effects in 2D amorphous plasticity: Results from a finite element model,” *J. Stat. Mech: Theory Exp.*, vol. 2015, no. 2, P02011, Feb. 2015. DOI: 10.1088/1742-5468/2015/02/P02011.
[106] Z. Zhen, D. Jun, and M. Evan, “Shear transformations in metallic glasses without excessive and predefinable defects,” *Proc. Natl. Acad. Sci.*, vol. 119, no. 48, e2213941119, 2022. DOI: 10.1073/pnas.2213941119.
[107] R. S. Lakes, *Viscoelastic Solids*. CRC press, 2017.
[108] T. Meidav, “Viscoelastic properties of the standard linear solid,” *Geophys. Prospect*, vol. 12, no. 1, pp. 80–99, 1964. DOI: 10.1111/j.1365-2478.1964.tb01891.x.
[109] T. Egami, “Atomic level stresses,” *Prog. Mater. Sci.*, vol. 56, no. 6, pp. 637–653, 2011. DOI: 10.1016/j.pmatsci.2011.01.004.
[110] C. Bernard et al., “Room temperature viscosity and delayed elasticity in infrared glass fiber,” *J. Eur. Ceram. Soc.*, vol. 27, no. 10, pp. 3253–3259, 2007. DOI: 10.1016/j.jeurceramsoc.2006.12.001.

[111] X. Jin, D. Lyu, X. Zhang, Q. Zhou, Q. Wang, and L. M. Keer, “Explicit analytical solutions for a complete set of the eshelby tensors of an ellipsoidal inclusion,” *J. Appl. Mech.*, vol. 83, no. 12, p. 121 010, 2016. DOI: 10.1115/1.4034705.

[112] L. Duffrène et al., “Generalized maxwell model for the viscoelastic behavior of a soda - lime - silica glass under low frequency shear loading,” *Rheol.Acta*, vol. 36, pp. 173–186, 1997. DOI: 10.1007/s003970050034.

[113] T. Rouxel, “Elastic properties and short-to medium-range order in glasses,” *J. Am. Ceram. Soc.*, vol. 90, no. 10, pp. 3019–3039, 2007. DOI: 10.1111/j.1551-2916.2007.01945.x.